NON-BOLTZMANN STATIONARY DISTRIBUTIONS AND NON-EQUILIBRIUM RELATIONS IN ACTIVE BATHS

A THESIS SUBMITTED TO
THE GRADUATE SCHOOL OF ENGINEERING AND SCIENCE
OF BILKENT UNIVERSITY
IN PARTIAL FULFILLMENT OF THE REQUIREMENTS FOR
THE DEGREE OF
MASTER OF SCIENCE
IN
PHYSICS

By
Aykut Argun
September 2016

NON-BOLTZMANN STATIONARY DISTRIBUTIONS AND NON-EQUILIBRIUM RELATIONS IN ACTIVE BATHS

By Aykut Argun

September 2016

We certify that we have read this thesis and that in our opinion it is fully adequate, in scope and in quality, as a thesis for the degree of Master of Science.

Giovanni Volpe(Advisor)

Gökhan Barış Bağcı

Seymur Jahangirov

Approved for the Graduate School of Engineering and Science:

Ezhan Karaşan
Director of the Graduate School

ABSTRACT

NON-BOLTZMANN STATIONARY DISTRIBUTIONS AND NON-EQUILIBRIUM RELATIONS IN ACTIVE BATHS

Aykut Argun
M.S. in Physics
Advisor: Giovanni Volpe
September 2016

Most natural and engineered processes, such as biomolecular reactions, protein folding, and population dynamics, occur far from equilibrium and, therefore, cannot be treated within the framework of classical equilibrium thermodynamics. Here, we experimentally study how some fundamental thermodynamic quantities and relations are affected by the presence of the non-equilibrium fluctuations associated with an active bath. We show, in particular, that, as the confinement of the particle increases, the stationary probability distribution of a Brownian particle confined within a harmonic potential becomes non-Boltzmann, featuring a transition from a Gaussian distribution to a heavy-tailed distribution. Because of this, non-equilibrium relations (e.g. Jarzynski equality, Crooks fluctuation theorem) cannot be applied. We show that these relations can be restored by using the effective potential associated with the stationary probability distribution. We corroborate our experimental findings with theoretical arguments.

Keywords: stochastic thermodynamics, non-equilibrium relations, active baths.

ÖZET

AKTİF BANYOLARDA BOLTZMANN DIŞI DURGUN DAĞILIMLAR VE DENGE DIŞI TERMODİNAMİK YASALARI

Aykut Argun
Fizik, Yüksek Lisans
Tez Danışmanı: Giovanni Volpe
Eylül 2016

Biyomoleküler reaksiyonlar, protein katlanması ya da populasyon dinamiği gibi birçok doğal ve tasarlanmış proses denge durumundan uzakta cereyan eder, dolayısıyla klasik termodinamik ile modellenemez. Bu çalışmada, bazı temel termodinamik niceliklerin ve denklemlerin aktif bir banyonun varlığından kaynaklanan denge dışı dalganalanmalardan nasıl etkilendiğini deneysel olarak inceliyoruz. Özellikle Brown parçacığının dar bir alana sıkıştırılması, durgun olasılık dağılımının Boltzmann dışına çıkmasına ve Boltzmann dağılımından ağır kuyruklu bir dağılıma geçişine sebep olmaktadır. Bu nedenle, denge dışı termodinamik yasaları (örneğin, Jarzynski denklemi ya da Crooks dalgalanma teoremi) bu sistemlere uygulanamaz. Bu problemin durgun olasılık dağılımını kullanarak elde edilen efektif bir potansiyel kullanılarak düzeltilebileceğini gösteriyoruz. Bu deneysel bulgularımızı teorik kanıtlar ile destekliyoruz.

Anahtar sözcükler: stokastik termodinamik, denge dışı termodinamik denklemler, aktif banyolar.

Acknowledgement

This research has been completed during my Master's studies. Here, I would like to thank to all people who has contributed to my motivation during the last two years.

First of all, I want to highlight the contribution of my family to my research as they have always been supportive about my academic goals. They have not judged a single decision I ever made in my life, some of which I believe looked pretty crazy from their picture. I know how much proud of me you are and I also know that I will overcome any problem in my life no matter how tough it is in order not to dissappoint you. I cannot tell how lucky I am to have you.

In addition to my family, I would like thank my close friends who have always supported me. Abdullah, we have spent 8 years together in Ankara and have shared a lot. I do not even know how to thank you, thanks for all of your support and friendship. In addition, I want to highlight the contributions of Mustafa, it was a pleasure for me to be your translator :) I am sorry to inform Murat that his efforts to distract me from science has not been successful, I am finally here at the last step of my Master. I want to thank Davut, Oguz, Bilal, Enes, Tugrul, Salih, Erion, Yusuf, Selim, Ali and Hakan for their support.

I also want to thank sincerely to all members of Soft Matter Lab. All of this would not have been possible if I have not been in such an amazing research group. Joining this group was one of the best decisions I ever made, not only because of the scientific productivity, but also because we had a wonderful social environment. As a person who have been in the group for over four years, I have witnessed the best of helpfulness and friendship. Also, our group has been quite active in terms of scientific events, we hosted one IONS and two COST action meetings in Ankara. As a Master student, I had the opportunity to participate in 4 COST action meetings and 2 international conferences, which provided me with a lot of experience and a good network. Particularly, I would like to thank Sabareesh and Sathya for helping me with all the experimental protocols that I

learned, Agnese for teaching me how to use Latex and helping us as a lab manager, Elif for taking care of administrative things, Tugba for tips regarding official documents, and Jalpa for providing feedback on my thesis. I also sincerely thank the rest of the group: Masoumeh, Alex, Mehdi, Fatemeh, Mite, Naveed, Geet, Merve, Ehsan, Falko, Serdar, Murad, Bora, Pascal, Yagmur and Muhammeds, thank you so much for all the unforgettable times we had. In addition, I highlight the contribution and support from my department, all of the faculty members and Fatma Gul.

I also want to highlight the contribution and support that I have received from my coauthors. Thanks Ali-Reza for introducing me experimental optics and working principles of light modulators. Thanks Ercag for his help regarding the bacteria production, I have learned a lot from him. I thank sincerely to Baris hoca, who has always supported my studies and appreciated so much that I generally felt overrated. He has been a very close friend with me apart from being a collaborator. Also, I want to thank to Seymur hoca, who participated in my defense as a committee member. It is a pleasure for me to have such a young and yet very bright scientist in my jury.

Finally, I would like to thank to my advisor. Dear Giovanni, I have spent a lot of time thinking a way to express how much I appreaciate your supervision, but I figured out that it is beyond my writing skills. Thanks for coming to Bilkent and contributing to my country...

Contents

List of Figures

Chapter 1

Introduction

In the 19^{th} century, classical thermodynamics had a major effect on development of industry and automation. A long journey of countless investigations began with an intense study of heat engines, highly stimulated by the development of the transportation sector after the industrial revolution. At the time, it was crucial to use vapor engines with the highest possible efficiency, and therefore, scientist looked for the limits that the nature had set via thermodynamic laws. The first and second laws of thermodynamics, as crucial cornerstones in classical thermodynamics, were discovered in a relatively short time interval [1].

One of the most significant steps forward in classical thermodynamics is the discovery of its relation with information in the mid 20^{th} century. Scientists found the thermodynamic limits of information-to-energy conversion and the costs of information erasure. These theories became extremely appealing especially after the computer industry got closer to these limits. For instance, heat dissipation in the processors is one of the biggest problems for hardware developers, which is directly connected to the Landauer's limit [2]. Landauer himself was a computer scientist but he is also considered to be one of the biggest contributors to the thermodynamics of information processing.

All of these thermodynamic relations arised from statistical physics and were

proven to be valid for macroscopic systems, where a system has a gigantic number of components or particles such that there are superabundant degrees of freedom therefore ensemble averaging for a system is reasonable. However, as soon as scientists had access to microscopic systems, they immediately realized that some of the fundemantal laws of thermodynamics do not always hold for such small systems. In 1993, for example, scientists observed that the 2^{nd} law of thermodynamics might be violated for small systems at short timescales. Nevertheless, the 2^{nd} law was shown to be correct in average [3].

Within the last two decades, as stochasticity is largely incorporated into thermodynamics, researchers have shown that not only the average values of thermodynamic quantities give us information about a system, but also fluctuations around the mean values for stochastic systems store significant amount of information about an irreversible microscopic process. It has been shown that these fluctuations have to follow certain statistical conditions. Therefore, we can extract equilibrium information from non-equilibrium data via repeating the measurement numerous times. These relations, such as Jarzynski equality [4], Crooks fluctuation theorem [5] and the integral fluctuation theorem [6], have been tested on various systems such as RNA stretching [7, 8], mechanical [9, 10] and colloidal [11] experiments. One of the key common point for all of these experiments is the fact that they were all thermalized with a heat reservoir.

Active systems, however; are generally considered to be instrinsically out-of-equilibrium [12, 13]. Whether particles in such active baths can be considered as equilibrium states is yet ambiguous. This ambiguity arises from the fact that the forces acting on a Brownian particle in an active bath are non-Markovian [14]. There have been studies where these systems can be generalized to equilibrium systems with effective temperatures [15, 16]. However, several studies showed that the resulting behaviour of such systems exhibit certain phenomena that are highly unlikely to be observed in a thermal equilibrium system with any possible effective temperature [17, 18]. Thus, it is an open and appealling question whether thermodynamic equilibrium conditions and non-equilibrium relations such as Crooks fluctuation theorem (CFT), Jarzynski equality (JE) and the integral fluctuation theorem (IFT) can be employed in an active bath.

In this work, we have analyzed and quantified the active noise associated with an active bath, which we realized experimentally by growing motile bacteria culture (*E.*coli). We report that when a particle is confined into a potential with large length scales, compared to the correlation length of active noise (i.e. persistence length), the particle's behaviour follows Boltzmann statistics with an effective temperature; thus, this case can then be treated as equilibrium. However, when we confine the particle into smaller length scales than the persistence length, the particle shows qualitatively different behaviour than the case of equilibrium and its distribution cannot be fitted to Boltzmann statistics with any possible effective temperatures. We conclude that at such scales, it is not possible to treat active bath systems as equilibrium systems.

After this step, we performed for the first time, non-equilibrium work measurements for a particle in an active bath. We drived an external optical potential and calculated the thermodynamic work applied to the particle and the heat exchange between the particle and the active bath. Following from these results, we have shown that in the non-Boltzmann regime, fluctuation theorems are no longer valid. Nevertheless, we report that non-equilibrium relations such as CFT, JE and IFT can be recovered by introducing an effective potential, which is estimated from the stationary distribution of the particle in the optical trap with imposing Boltzmann distribution.

The rest of this thesis includes five chapters and a conclusion. I will first give a summary on microthermodynamics and stochastic thermodynamics (chapter 2). Then I will give a detailed description of fluctuation theorems with numerical illustrations along with experimental verifications in the literature (chapter 3). I will then introduce the fundamental properties of an active matter system (chapter 4). Finally, I will share my results related to the stationary distributions of a particle in an active bath (chapter 5) and non-equilibrium measurements (chapter 6) before the conclusion.

To sum up, in this thesis, I report violations of some cornerstones of classical thermodynamics such as the Boltzmann relation as well as some fundamental fluctuation theorems of thermodynamics in active baths. This outcome arises

from the fact that in an active bath, there is time-correlated (non-Markovian) noise associated with the active bath which we characterize with our experimental data. We also show that these violated relations can still be recovered using effective potentials that would satisfy Boltzmann relation.

Chapter 2

Introduction to Stochastic Thermodynamics

One of the most fundamental concepts in thermodynamics, and indeed one of the earliest, is reversibility. It was introduced by Sadi Carnote in 1824 within his studies on heat engines, which later led to the 2nd law of thermodynamics [19, 20]. A reversible process occurs when a thermodynamic protocol is applied infinitely slow such that there are no permanent changes in the universe, i.e., one can revert the system to its initial conditions if the reverse protocol is followed. On the other hand, an irreversible process occurs in a finite time and therefore results in heat dissipation in the medium. This is a permanent change because once the heat is dissipated to the heat bath that is in contact with our system, there is no way to collect that heat back without an additional cost of energy. The second law of thermodynamics, which is also described as 'time's arrow' acquired its quantitative form after the concept of entropy was proposed:

$$dS \geq 0 \tag{2.1}$$

where dS denotes the total entropy change in the universe. If one considers the entropy of a system (S_{sys}) and the entropy of the environment (S_{env}) separately, $S = S_{sys} + S_{env}$. Then Eq. (2.1) becomes:

$$dS_{sys} + dS_{env} \geq 0. \tag{2.2}$$

If we combine the above equation with the 1st law ($dW = dU + dQ$) and the definition of free energy ($dF = dU - TdS_{sys}$) we end up with a different version of the second law [21]:

$$dW \geq dF. \tag{2.3}$$

Eq. (2.3) states that, in any thermodynamic process, the work applied on the system has to be greater than or equal to the change in free energy. Therefore, free energy acts as a lower bound to the amount of work to be applied in a thermodynamic process, or an upper bound to the amount of extracted work when the change in free energy is negative.

The difference between the work done and the change in free energy is called dissipated work [1]:

$$dW_{dis} = dW - dF \geq 0 \tag{2.4}$$

In reality, not only the work we apply during a thermodynamic process, but also the fluctuations of the work applied contain information about the properties of the initial and final equilibrium states, which is going to be discussed in detail in chapter 3. In this chapter, I will give an overview about stochastic thermodynamics and the role of fluctuations on the 2nd law of thermodynamics (Eq. (2.3)).

2.1 Thermodynamics in the microscopic world

In this section, I discuss how fundamental thermodynamic quantities are calculated within the context of stochastic thermodynamics. All the thermodynamic relations and fluctuation theorems are discussed in this context. Also, the mathematical notation that is introduced in section will be consistently used in the rest of this thesis.

A micron-sized particle immersed in a liquid, which is called a Brownian particle, is assumed to be in contact with a thermal bath if the liquid has well-defined and constant temperature. Because of the random collisions between the particle and liquid molecules, this particle is subject to a stochastic force named thermal noise. Therefore, the resulting equation of motion reads [22, 23]:

$$m\frac{d^2x}{dt^2} = -\gamma\frac{dx}{dt} + \sqrt{2k_BT\gamma}W_x(t) \tag{2.5}$$

where γ represents the viscosity of the medium, k_B is the Boltzmann constant, T is the temperature of the liquid, and $W_x(t)$ represents the Gaussian white noise associated with the stochasticity of the system. Without losing any generality, we will mostly be dealing with one dimension only (the $x-$axis). All of the equations we are going to deal with are also valid for $y-$ and $z-$ axes, but the equations are separable as the thermal noise components are independent.

2.1.1 Solution of the Langevin equation and derivation of the Boltzmann distribution in a thermal bath

Consider a Brownian particle confined within a potential well $U(x)$. In this case, the particle's equation of motion will have the form:

$$m\frac{d^2x}{dt^2} = -\gamma\frac{dx}{dt} - \frac{dU(x)}{dx} + \sqrt{2k_BT\gamma}W_x(t) \tag{2.6}$$

For most micron-sized Brownian particles immersed in watery solutions, as the viscous forces are dominant over the inertial forces, the inertial term ($m\ddot{x}$) can be neglected [24]. Therefore, we can make use of the overdamped version of Eq. (2.6):

$$\frac{dx}{dt} = -\frac{1}{\gamma}\frac{dU(x)}{dx} + \sqrt{2k_BT/\gamma}W_x(t) \tag{2.7}$$

Although there are significant challenges to numerically solve stochastic differential equations, particularly with the infinite variance of white noise, it is possible to solve Eq. (2.7) with finite difference methods [25, 26, 27]. By numerically simulating Eq. (2.7), I obtained trajectories for various potentials, which are shown in Fig. 2.1(d), Fig. 2.1(e) and Fig. 2.1(f).

It is also possible to solve Eq. (2.7) analytically by using the Fokker-Planck equation [28]:

$$\partial_t P(x,t) = \frac{1}{\gamma}\partial_x\left(\frac{dU(x)}{dx}P(x,t)\right) + \frac{k_BT}{\gamma}\partial_x^2 P(x,t) \tag{2.8}$$

$P(x,t)$ denotes the probability density function of the particle as a function of x and t. We are looking for an equilibrium distribution after the particle spends enough time to thermalize in the potential for which $\partial_t P(x,t) = 0$, i.e., when P is a function of x only. When this is the case, the left handside of the Eq. (2.8) vanishes and we obtain:

$$-\partial_x\left(\frac{dU(x)}{dx}P_{eq}(x)\right) = k_BT\partial_x^2 P_{eq}(x)$$

$$-\frac{dU(x)}{dx}P_{eq}(x) = k_BT\partial_x P_{eq}(x) + C$$

$$P_{eq}(x) = C\exp\left(-\frac{U(x)}{k_BT}\right) \tag{2.9}$$

where $C = \frac{1}{Z} = (\int \exp\left(-\frac{U(x)}{k_B T}\right))^{-1}$ can be found via normalization with the partition function $Z = \int \exp\left(-\frac{U(x)}{k_B T}\right)$. Therefore, this proves that a Brownian particle subject to thermal noise will reach the Boltzmann distribution when it is confined in any stable potential well. This relation is also verified numerically from the distribution of the data obtained by simulating Eq. (2.7) for various potentials and shown in Fig. 2.1(g), Fig. 2.1(h) and Fig. 2.1(i).

Satisfying Boltzmann distribution, however, is not enough for a system to be considered in equilibrium. The system should not have any probability current, therefore the probability of forward and backward transitions for any two states that are accesible should be the same. Assuming we have two states S_1 and S_2 with energies U_1 and U_2, the transition rates in both directions should be the same:

$$p_1(t)p\left[S_2(t+\Delta t) \mid S_1(t)\right] = p_2(t)p\left[S_1(t+\Delta t) \mid S_2(t)\right]$$

$$\exp\left(\frac{-U_1}{k_{\mathrm{B}}T}\right) p\left[S_2(t+\Delta t) \mid S_1(t)\right] = \exp\left(\frac{-U_2}{k_{\mathrm{B}}T}\right) p\left[S_1(t+\Delta t) \mid S_2(t)\right] \quad (2.10)$$

this condition is named detailed balance [1] and requires equal rate of transitions between the two states. A consequence of this relation is the ratio of conditional transition probabilities between two equilibrium states:

$$\frac{p\left[S_2(t+\Delta t) \mid S_1(t)\right]}{p\left[S_1(t+\Delta t) \mid S_2(t)\right]} = \exp\left(\frac{-(U_2-U_1)}{k_{\mathrm{B}}T}\right) \quad (2.11)$$

We will make use of this relation in the next chapter when I will give the derivation of Crooks fluctuation theorem.

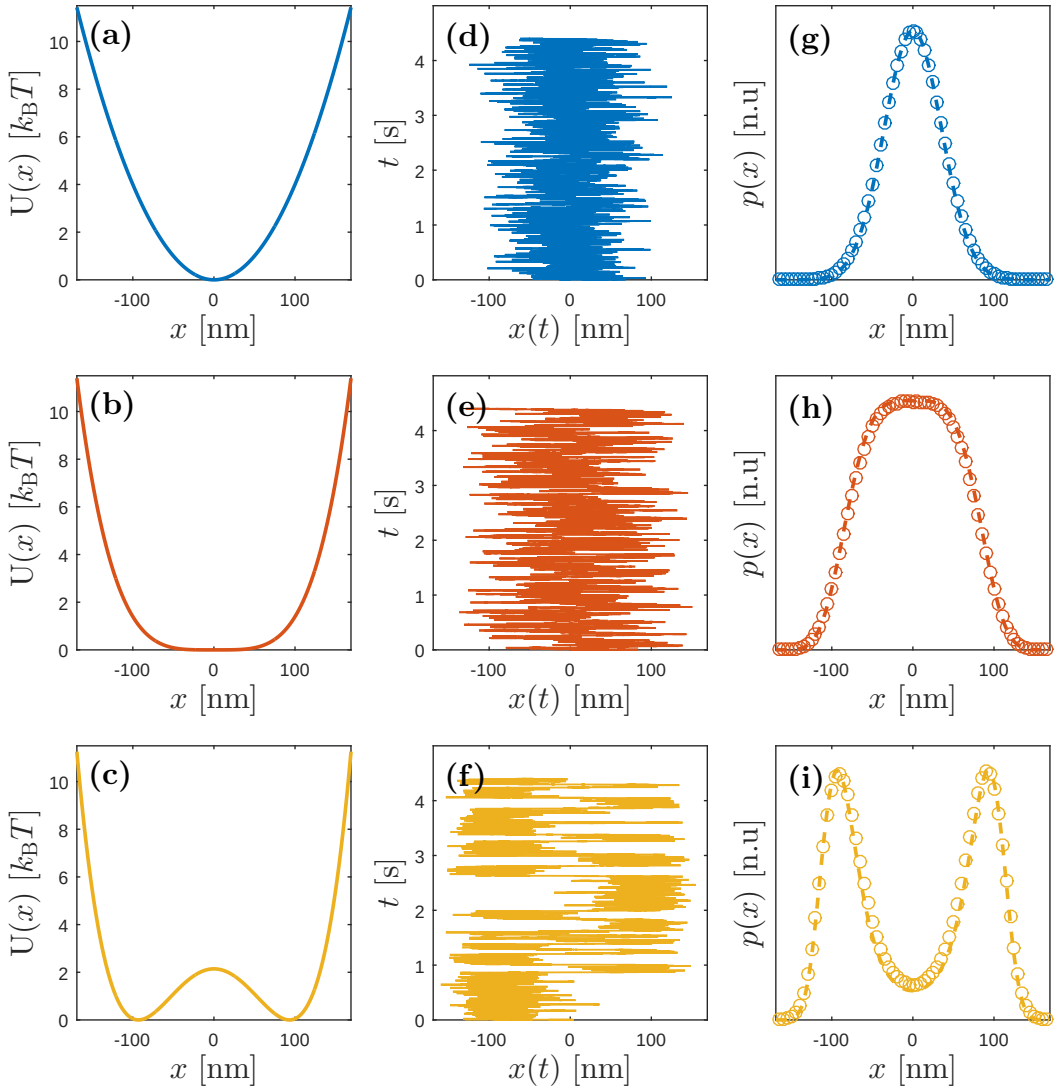

Figure 2.1: **Demonstration of Boltzmann distribution for a confined Brownian particle. (a)**,**(b)** and **(c)**: Various confining potentials such as a harmonic potential (a), a quartic potential (b), and a bistable potential (c) are shown. **(d)**, **(e)** and **(f)**: Corresponding sample trajectories of a colloidal particle with radius $R = 1$ μm under the confining potentials shown in (a), (b), and (c), respectively. Trajectories are obtained by numerically solving Eq. (2.7). Matlab code is provided in the appendix B. **(g)**, **(h)** and **(i)**: Resulting numerical probability distributions (circles) of the particles obtained from trajectories, which are in perfect agreement with the theoretical probability ditributions given by Eq. (2.9)

2.1.2 Stochastic energetics

In classical thermodynamics, we do not apply work on a system unless we externally control a confinement parameter of the system [1]. For example, for an ideal gas, we do not apply work unless we change its volume. During such a thermodynamic process, there is only heat exchange between the bath and the system.

For microscopic systems, however, how to quantify the heat exchange and work applied on a Brownian particle in a stochastic system has only recently been sorted out. Sekimoto integrated the principles of thermodynamics with stochastic systems which are driven by Langevin equations [29, 30]. He also discussed the first law of thermodynamics at microscopic scales within the context of stochastic energetics.

Let's consider a Brownian particle confined in a potential $U(x)$, which is only a function of the position of the particle and kept constant over time. As we do not change the confinement parameter of the system, we do not apply any work on the particle. Due to fluctuations, however, there is always heat exchange between the particle and the bath. Since there is no work applied, all the change in the particle's potential energy comes from the surrounding heat bath:

$$dU = dQ$$

Therefore, the heat transferred from the thermal bath to the particle can be written as:

$$dQ = \frac{\partial U(x)}{\partial x} dx \tag{2.12}$$

Unlike macroscopic systems, heat exchange between the particles and heat bath cannot be isolated for Brownian particles as they are immersed in liquid solutions and they constantly collide with surrounding molecules. Thus, it is not trivial to operate an adiabatic process in such systems [31].

Now, assume that our external potential is not kept constant, but depends on

a control parameter $\lambda(t)$, which is an arbitrary function of time. Then, we are also going to apply work on the particle through the variation of the potential:

$$U = U(x, \lambda(t))$$

$$dU = \underbrace{\frac{\partial U(x, \lambda(t))}{\partial x} dx}_{dQ} + \frac{\partial U(x, \lambda(t))}{\partial \lambda} d\lambda \tag{2.13}$$

The first law of thermodynamics states [30]:

$$dU = dQ + dW \tag{2.14}$$

Combining Eq. (2.14) and Eq. (2.13) yields:

$$dW = \frac{\partial U(x, \lambda(t))}{\partial \lambda} d\lambda \tag{2.15}$$

Therefore, we apply work on a Brownian particle when we change the potential parameters. The reversibility condition for such a process will be discussed soon.

Example 2.1: Isochoric heating

The thermodynamic process involving the heating of the medium surrounding a particle held in a harmonic trap can be illustrated by the following example. Consider a Brownian particle with radius ($R = 1$ μm) is immersed in a liquid and the temperature of the medium is raised from $T_i = 50$ K to $T_f = 500$ K over 5 seconds while the particle is confined in a constant harmonic potential:

$$U(x) = \frac{1}{2}kx^2$$

Since the potential parameters are kept constant, we do not apply any work on the system but we only heat the surrounding bath; this is an illustration of an isochoring heating in stochastic thermodynamics. Therefore, the Langevin equation that will govern the non-equilibirum dynamics for this specific process will take the form:

$$\frac{dx}{dt} = -\frac{1}{\gamma}kx + \sqrt{2k_BT(t)/\gamma}W_x(t) \tag{2.16}$$

This equation is simulated and a sample resulting trajectory is shown in Fig. 2.2(a). The average potential energy of the Brownian particle in this harmonic trap can easily be calculated and shown to be in agreement with the equipartition theorem [1]:

$$\langle U(x)\rangle = \int p(x)U(x)dx = \frac{k_BT}{2} \tag{2.17}$$

Since for our example $T_f = 10T_i$, the final probability distribution of the particle will be expanded (shown in Fig. 2.2(b)) and change in its potential energy will be $\langle \Delta U(x)\rangle = \frac{k_B(T_f - T_i)}{2} = \frac{9k_BT_i}{2}$. This average is verified by my numerical example and shown in Fig. 2.2(d), but it is important to note here that the fluctuations are very important in stochastic systems as the heat exchange in a single realization has a completely different profile than the average (Fig. 2.2(c)).

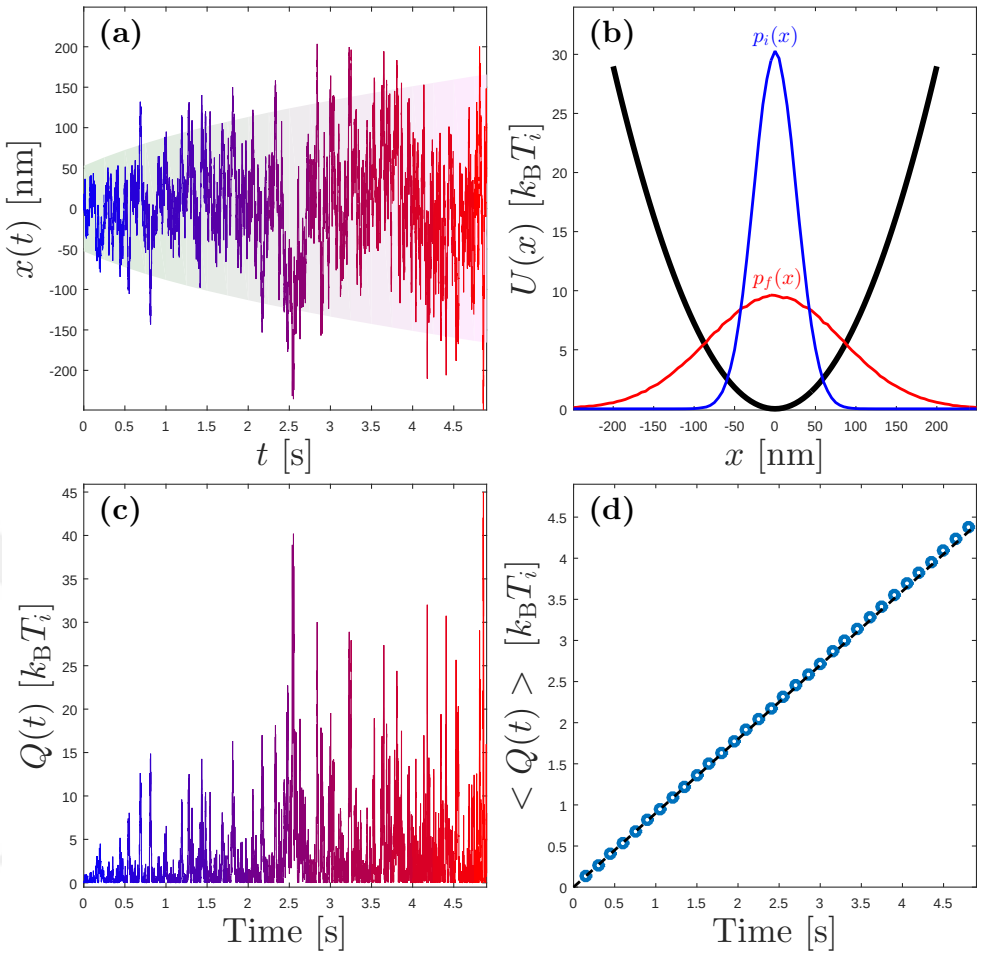

Figure 2.2: **Illustration of an isochoric process.** **(a)**: Sample trajectory of a Brownian particle in a harmonic trap which undergoes an isochoric heating as described in Example 2.1. The particle's trajectory is shown and color-coded with the temperature as a function of time. The red color represents hot and the blue represents cold. The background shading represents particle's standard deviation in the trap as a function time. **(b)**: Constant potential energy is shown. Also, the particle's initial and final position distributions within this trap are shown. **(c)**: Heat exchange between the bath the particle. Note that the fluctuations play a very important role and they are much bigger than the average heat transfer, shown in (d). **(d)**: The average heat transfer (circles) and the change in particle's average potential energy (dashed line) are shown. Since this process is operated during a long enough time (5 s), this two average quantities match. The simulation codes are provided in appendix B.

Example 2.2: Isothermal compression

In this numerical example, we will explore how work is applied on a Brownian particle during a non-equilibrium process. Unlike Example 2.1, here we keep the temperature constant, but change the stifness of the confining trap from $k_i = 1$ pN/μm to $k_f = 10k_i = 10$ pN/μm. This protocol is illustrated in Fig. 2.3(a). During such a process, since the temperature is kept constant, the average potential energy of the particle will not change due to equipartition theorem (Eq. (2.17)). Unlike in a macroscopic process, in a microscopic thermodynamic process, the energy of the system will always be fluctuating during a single realization due to the strong coupling between the particle and heat bath. The resulting Langevin equation during such a process will then take the form:

$$\frac{dx}{dt} = -\frac{1}{\gamma}k(t)x + \sqrt{2k_BT/\gamma}W_x(t) \tag{2.18}$$

Several resulting sample trajectories from numerical simulations are shown in Fig. 2.3(c). Also, the work done on the particle during these realizations is calculated using Eq. (6.8) and shown in Fig. 2.3(d). Note that again in single realizations, fluctuations play a crucial role and result in significant deviations from the average work applied.

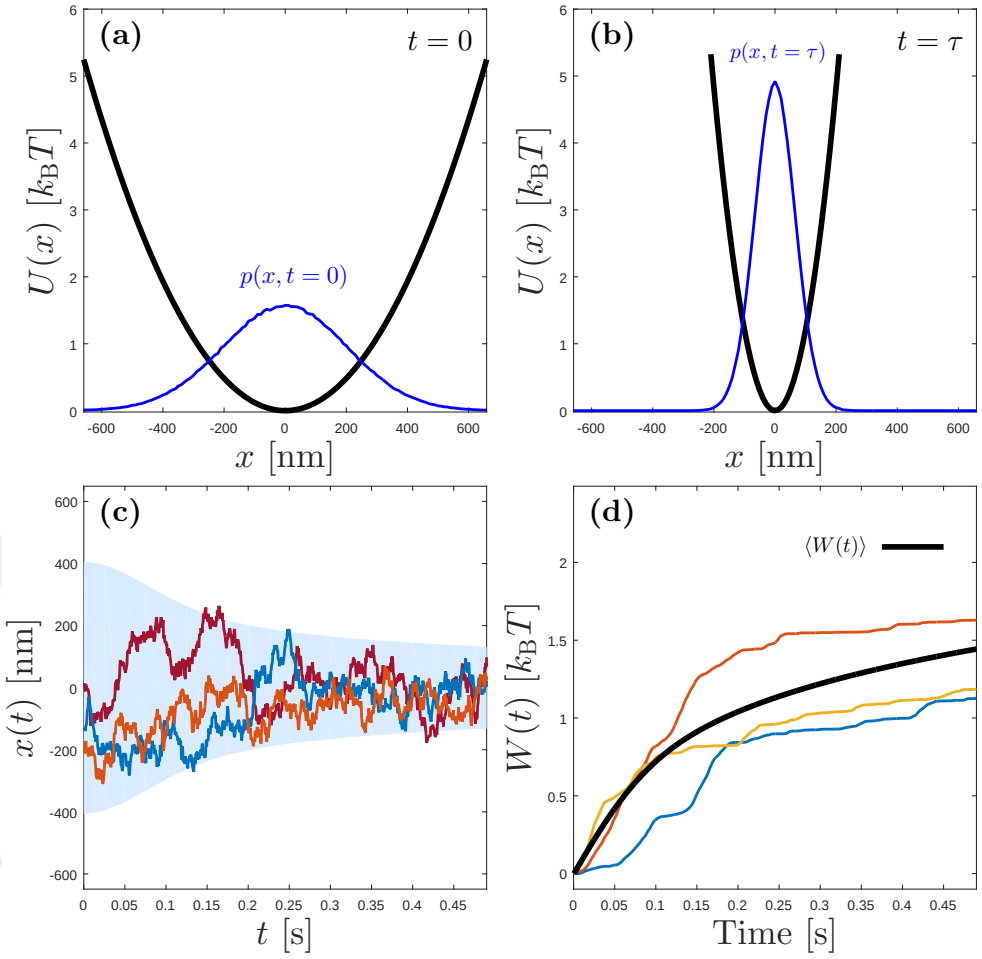

Figure 2.3: **Illustration of an isothermal process.** **(a)**: The initial potential well and the initial probability distribution of the particle are shown. **(b)**: The final potential and the final probability distribution of the particle are shown, the process takes $\tau = 0.5$ s time. **(c)**: Several sample trajectories of a Brownian particle in a harmonic trap which undergoes an isothermal compression as described in Example 2.2. Note that different realizations of the same non-equilibrium protocols yield significantly different trajectories. The particle's standart deviation over time is calculated over 1000000 realizations and indicated with the light blue background shading. **(d)**: Work done on the trajectories that are shown in (c). Average work done is also shown by black line. Note that in such a stochastic process, fluctuations around the mean value are significant. The simulation codes which generated these results are provided in appendix B.

2.1.3 Stochastic heat engines

The first thermodynamic heat engine was introduced by Sadi Carnote in 1824 [19]. Starting with this pioneering discovery, researchers heavily focused on thermodynamics and heat engines. As the development in nanotechnology enabled scientists to work with smaller systems, micro-thermodynamics emerged. Scientists discovered methods to convert thermal energy into work at the micro-scale by using Brownian ratchets [32] inspired by nature [33].

The development of stochastic thermodynamics [34, 35] permitted scientists to experimentally discover microscopic thermodynamics. Eventually, stochastic heat engines with micron-sized dimensions were experimentally realized [36, 37, 38, 39]. The first stochastic heat engine that works between two temperatures was theoritically proposed and examined by Schmiedl and Seifert in 2007 [40]. They modeled a stochastic heat engine which mimics the industrial Stirling engine [41] that consists of 4 separate processes:

1. Isochoric heating, which is demonstrated in Example 2.1 (Fig. 2.2)
2. Isothermal expansion, reverse of Example 2.2 (Fig. 2.3)
3. Isochoric cooling, reverse of Example 2.1 (Fig. 2.2)
4. Isothermal compression, Example 2.2 (Fig. 2.3)

This model was experimentally realized by Blickle and Bechinger in 2012 [36]. They realized the harmonic potential with the help of optical tweezers [42] and instant heating of the viscinity of the Brownian particle with a laser absorption technique [43]. The experimental protocol is demonstrated in Fig. 2.4, which is adapted from the original paper [36].

After the first realization of a micron-sized heat engine, several colloidal heat engines were also realized by experimentalists such as a Brownian Carnot engine [37] and microscopic steam engine [38].

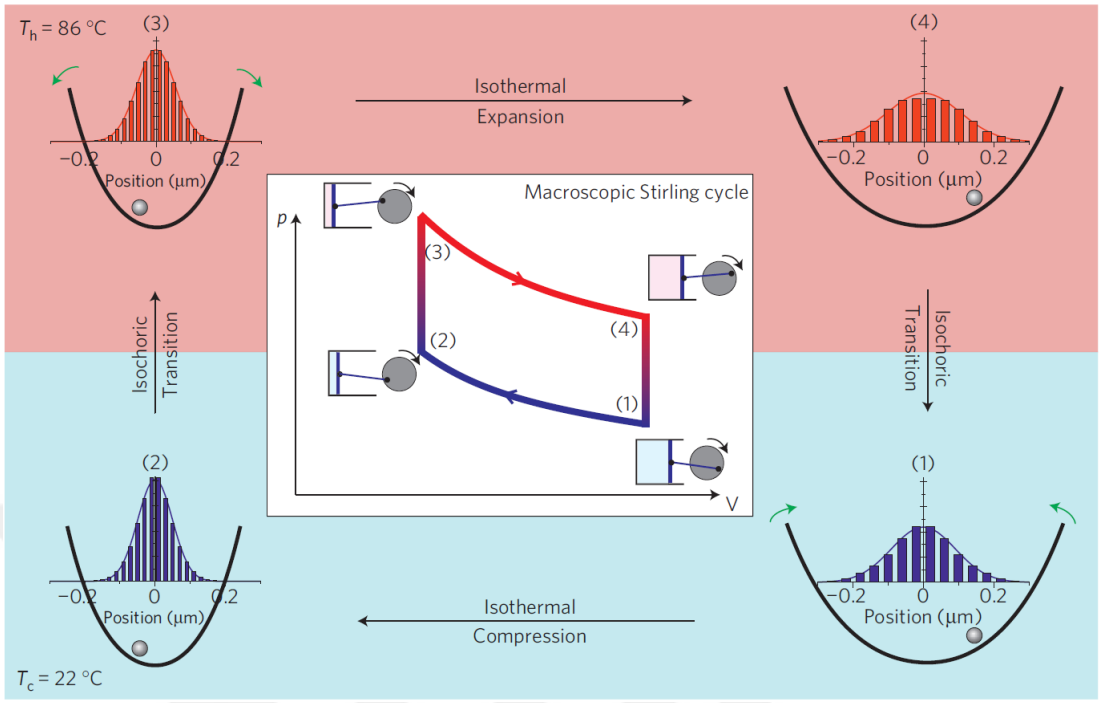

Figure 2.4: **Schematic comparison of a macroscopic Stirling cycle and its realization in a colloidal system.** (1) The particle is initially in a low-stiffness trap and the system is initially kept at $T_c = 22$ °C. Then the stiffness is increased to operate an isothermal compression at low temperature and the cycle reaches (2). This process is followed by an isochoric heating, where the stiffness is kept constant but the temperature is increased to $T_h = 86$ °C and the cycle reaches (3). After that, isothermal expansion is operated by decreasing the stiffness back to its original value while the temperature is kept constant at T_h, system is reached (4) at the end of this process. Finally, the system is brought back to its initial state by an isochoric cooling. Histograms represent the equilibrium distributions of the particle at each state inside the trap. Inset: The corresponding macroscopic Stirling engine represented with a $P - V$ diagram. Adapted from [36].

2.2 Irreversibility, second law of thermodynamics and the role of fluctuations in small systems

For a Brownian particle with stationary probability distribution function $P(x,\lambda) = C\exp\left(-\frac{U(x,\lambda)}{k_BT}\right)$, the free energy can be written as:

$$F = -k_BT\ln(Z) \tag{2.19}$$

For a reversible process, the dissipated work can then be written as:

$$dW_{dis} = dW - dF = \frac{\partial U(x,\lambda(t))}{\partial\lambda}d\lambda - \frac{k_BT}{Z}\frac{\partial Z}{\partial\lambda}d\lambda$$

Substituting $Z = \int\exp\left(-\frac{U(x)}{k_BT}\right)$ into the above equation yields:

$$dW_{dis} = d\lambda\left[\frac{\partial U(x,\lambda(t))}{\partial\lambda} - \frac{1}{Z}\int\exp\left(-\frac{U(x,\lambda)}{k_BT}\right)\frac{\partial U(x,\lambda(t))}{\partial\lambda}dx\right] \tag{2.20}$$

Note that the first term inside the square bracket is not deterministic, rather it depends on the position of the particle at the given time. Therefore, the dissipated work as well as the work applied to a Brownian particle during a non-equilibrium process is stochastic and trajectory-dependent. Nevertheless, we can still show that there is no dissipated work if the process is reversible.

Assume that the control parameter is changing infinitely slowly. In such case, we can assume that the particle is under the same trapping potential for a very long time. Therefore, the infinitesimal dissipated work will take the form:

$$dW_{dis} = d\lambda \left[\frac{1}{d\lambda/\dot{\lambda}} \int_0^{d\lambda/\dot{\lambda}} \frac{\partial U(x,\lambda(t))}{\partial \lambda} dt - \frac{1}{Z} \int \exp\left(-\frac{U(x,\lambda)}{k_B T} \right) \frac{\partial U(x,\lambda(t))}{\partial \lambda} dx \right] \tag{2.21}$$

Note that the first term inside the square brackets is the time average and the second term is the space average of the function $\frac{\partial U(x,\lambda(t))}{\partial \lambda}$. In the limit where $\dot{\lambda}$ goes to zero, these two terms will be equal to each other due to ergodicity, and therefore; we will not have any dissipated work. Thus:

$$\lim_{\dot{\lambda} \to 0} dW_{dis} = 0 \tag{2.22}$$

This implies that, just like in the classical thermodynamics, a reversible thermodynamic process can be obtained provided that the system parameters are changed infinitely slowly.

The second law of thermodynamics states that no thermodynamic process can result in a decrease in the total entropy of the universe. This was proven to be true for macroscopic systems, but it was shown by Evans that this law does not always apply to small systems [3]. They performed computational studies on a liquid under external shear and concluded that due to fluctuations comparable to the system's thermal energy, negative entropy production can be observed for small systems at small timescales. This phenomenon was investigated by scientists on different systems within the following years and yielded consistent results [44, 45, 46, 47]. Even though the second law does no longer hold when the system has a finite number of degrees of freedom, according to fluctuation theorem the second law of thermodynamics still holds on average:

$$\langle dW \rangle \geq dF \tag{2.23}$$

This phenomenon is also visible in the numerical illustration of Example 2.2. The free energy of a Brownian particle is calculated according to Eq. (2.19) and

compared with work values in single realizations. In Fig. (2.3)(d), we see that the applied work can be smaller than the change in free energy in a single realization of an isothermal process, but it is still greater in average. Of course, not only the mean values, but also the fluctuations around these average values store significant information about thermodynamic systems, which will be discussed in more detail in Chapter 3.

Chapter 3

Fluctuation Theorems

In the previous chapter, thermodynamic quantities for microscopic systems are discussed. I have shown with numerical examples that for a microscopic particle that undergoes an irreversible process, thermal fluctuations give rise to significant deviations from expected values. Even though the second law still holds on average, statistical fluctuations become increasingly crucial for small systems.

So far, only the mean values of the quantities in micro-thermodynamics have been dealt with in this thesis. Although being accurate and useful, this framework is not complete. In 1997, Jarzynski pointed out that the fluctuations around mean values contain significant information. He concluded that the work distribution for a system that is driven out of equilibrium should satisfy [4, 48]:

$$\langle e^{-(W-\Delta F)/(k_{\mathrm{B}}T)} \rangle = 1 \tag{3.1}$$

where $\langle \cdot \rangle$ represents ensemble average and ΔF denotes the change in the free energy of the system.

For a microscopic system, the second law of thermodynamics is not always true, but it still holds on average. This is because the trajectories that result in positive entropy production are more likely to occur than their time-reversed versions.

Crooks stated that this rate of probabilities of observing the same quantity of positive and negative entropy production under time reversal is exponentially proportional to the production of entropy along the forward trajectory [5]:

$$\frac{P_F(+\Delta S)}{P_R(-\Delta S)} = e^{+\Delta S} \tag{3.2}$$

Also, he showed that for microscopically reversible Markovian systems, probability rates of observing the same forward and backward trajectories under time-reversal in an arbitrary process are given by [49]:

$$\frac{P(x(t), \lambda(t))}{P(\tilde{x}(t), \tilde{\lambda}(t))} = e^{-\beta Q} \tag{3.3}$$

where $P(x(t), \lambda(t))$ denotes the probability of observing a trajectory $x(t)$ under the protocol $\lambda(t)$, $P(\tilde{x}(t), \tilde{\lambda}(t))$ denotes that for the time reversed trajectory under the time-reversed protocol $\tilde{\lambda}$ and Q denotes the heat exchange between the particle and the heat bath along the forward protocol.

An important consequence of Eq. (3.3) is the work fluctuation theorem, which is valid if the system is initially thermalized [5]:

$$\frac{P_F(+W)}{P_R(-W)} = e^{-\beta(W-\Delta F)} \tag{3.4}$$

which also implies Jarzynski equality (Eq. 3.1). After these two relations, many other fluctuation theorems have been developed such as the Hatano-Sasa relation [50] and the Hummer-Szabo formula [51].

As the theoretical framework of stochastic thermodynamics developed [29, 52], other non-equilibrium relations have also been formulated [53, 54, 55, 56]. In this section, along with Crooks fluctuation theorem and Jarzynski relation, I am going to be particularly focusing on the integral fluctuation theorem [6, 57]:

$$\left\langle \exp\left(\beta Q - \log \frac{p(x_0)}{\tilde{p}(\tilde{x_0})}\right)\right\rangle = 1 \tag{3.5}$$

Unlike Eq. (3.1) and Eq. (3.4), Eq. (3.5) does not require initial equilibrium. All of these non-equilibrium relations attracted great interest from experimentalists and have been tested with experiments [7, 8, 58, 59, 11, 60, 61, 62, 9, 10, 63, 64].

In the rest of this chapter, I will explain Crooks fluctuation theorem, Jarzynski equality and the integral fluctuation theorem in detail with theoretical derivations and numerical exemplifications.

3.1 Crooks Fluctuation Theorem

In this section, I will explain in detail how Crooks obtained [49] Eq. (3.3) for Markovian systems and how this equation leads to Eq. (3.4) [5]. Then, I will illustrate this relation with numerical realizations under arbitrary non-equilibrium thermodynamic processes. Finally, I will conclude highlighting the first experimental realization of this relation.

Consider a Brownian particle in a thermal bath driven by an overdamped Langevin equation. Such a system is called Markovian as the particle's future trajectory has no dependence on its history. Consider a Brownian particle which is held initially in a potential given as:

$$U(x) = U(x, \lambda_0) \tag{3.6}$$

where λ_0 is the initial value of a control parameter that can be driven externally. We start changing this control parameter at $t = t_0$ and end the process at $t = t_N$. Without losing any generality, we can change $\lambda(t)$ in a discrete manner:

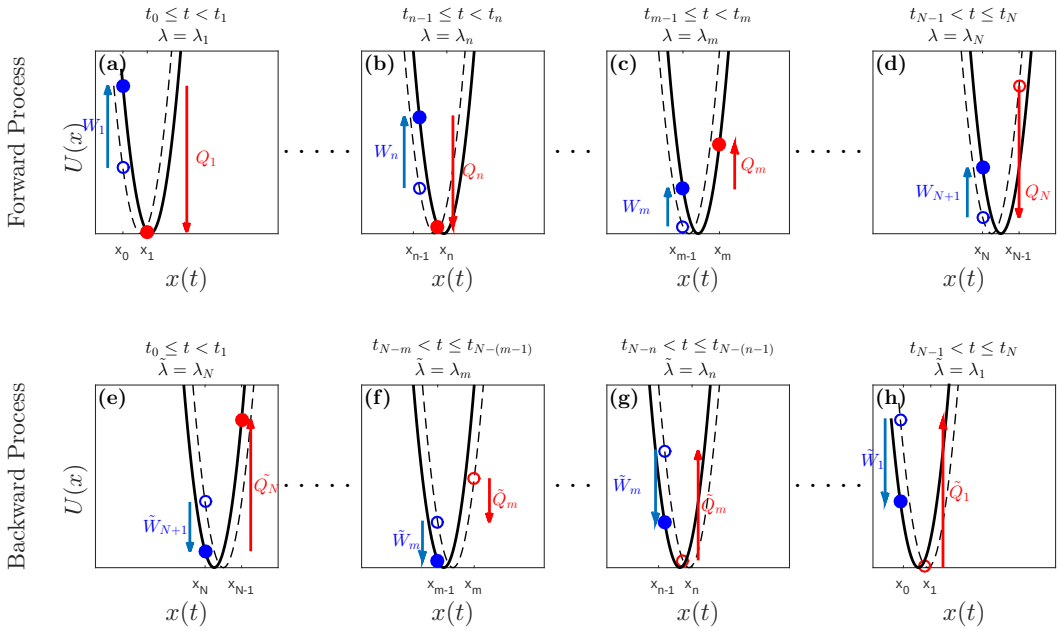

Figure 3.1: **The same forward and backward trajectories under time reversal in a non-equilibrium process.** The process starts with changing λ_0 to λ_1 at $t = t_0$. Then at each t_i, the control parameter is changed to λ_{i+1}. The titles indicate the time interval of each heat exchange and the control parameter during the same time. The time when the change in control parameter occurs is represented with equality. If the change of control parameter occurs after the heat exchange, the initial position of the particle is shown by red hollow circles. If the change of control parameter occurs before the heat exchange, the final position of the particle is shown by red disks. (a) corresponds to initiation of the process, (b) and (c) correspond to arbitrary intermediate steps, (d) corresponds to conclusion of the process. The reverse protocol is also shown in the same manner in (e),(f),(g) and (h), respectively. Note that $\tilde{W}_i = -W_i$ and $\tilde{Q}_i = -Q_i$ for the corresponding forward and backward steps.

$$\Lambda_F \equiv \lambda_0 \underset{t=t_0}{\Longrightarrow} \lambda_1 \cdots \lambda_n \underset{t=t_n}{\Longrightarrow} \lambda_{n+1} \cdots \lambda_N \underset{t=t_N}{\Longrightarrow} \lambda_{N+1} \quad . \tag{3.7}$$

The limit $N \to \infty$ corresponds to the continous case. We denote a certain trajectory, X as follows:

$$X = X\left(x_0(t_0), x_1(t_1), ...x_n(t_n).....x_{N-1}(t_{N-1}), x_N(t_N)\right) \tag{3.8}$$

The process begins at time $t = t_0$, when the control parameter is changed from λ_0 (dashed line) to λ_1 (solid line) as shown in Fig. 3.1(a), when W_1 work (blue arrow) is applied on the particle. Then the particle fluctuates inside the potential under control parameter λ_1 until $t = t_1$ while exchanging Q_1 heat (red arrow) with the heat bath. This process is iterated similarly, two intermediate steps are shown in Fig. 3.1(b) and Fig. 3.1(c). Finally, the particle reaches its final position x_N at $t = t_N$ having exchanged Q_N (red arrow) amount of heat with the bath, when we change λ_N (dashed line) to λ_{N+1} (solid line) and thus apply W_{N+1} (blue arrow) amount of work, shown in Fig. 3.1(d).

Given that the particle is initially at x_0 at $t = t_0$, the probability of observing the trajectory X can be written a product of conditional probabilities:

$$P_{\mathrm{F}}(X) = p\left[x_1(t_1) \mid x_0(t_0)\right]_{\lambda_1} \cdots p\left[x_n(t_n) \mid x_{n-1}(t_{n-1})\right]_{\lambda_n} \cdots p\left[x_N(t_N) \mid x_{N-1}(t_{N-1})\right]_{\lambda_N} \tag{3.9}$$

Now consider we operate the time-reversed protocol Λ_R, which starts with λ_{N+1} and ends with λ_0, opposite to Λ_F:

$$\Lambda_B \equiv \lambda_{N+1} \underset{t=t_0}{\Longrightarrow} \lambda_N \cdots \lambda_{n+1} \underset{t=t_n}{\Longrightarrow} \lambda_n \cdots \lambda_1 \underset{t=t_N}{\Longrightarrow} \lambda_0 \quad . \tag{3.10}$$

Let us find out the probability to observe the reversed trajectory under the reversed protocol. Similar to Eq. (3.9), we can express this probability given that the particle initially starts at x_N:

$$P_{\mathrm{R}}(\tilde{X}) = p\left[x_{N-1}(t_{N-1}) \mid x_N(t_N)\right]_{\lambda_N} \cdots p\left[x_n(t_n) \mid x_{n-1}(t_{n-1})\right]_{\lambda_n} \cdots p\left[x_0(t_0) \mid x_1(t_1)\right]_{\lambda_1} \tag{3.11}$$

$$= p\left[x_0(t_0) \mid x_1(t_1)\right]_{\lambda_1} \cdots p\left[x_n(t_n) \mid x_{n-1}(t_{n-1})\right]_{\lambda_n} \cdots p\left[x_{N-1}(t_{N-1}) \mid x_N(t_N)\right]_{\lambda_N} \tag{3.12}$$

Now we can calculate the rate of the probabilities of observing the time reversed

trajectory under the time reversed protocol:

$$\frac{P_{\mathrm{F}}(X)}{P_{\mathrm{R}}(\tilde{X})} = \frac{p\left[x_1(t_1) \mid x_0(t_0)\right]_{\lambda_1}}{p\left[x_0(t_0) \mid x_1(t_1)\right]_{\lambda_1}} \cdots \frac{p\left[x_n(t_n) \mid x_{n-1}(t_{n-1})\right]_{\lambda_n}}{p\left[x_n(t_n) \mid x_{n-1}(t_{n-1})\right]_{\lambda_n}} \cdots \frac{p\left[x_N(t_N) \mid x_{N-1}(t_{N-1})\right]_{\lambda_N}}{p\left[x_{N-1}(t_{N-1}) \mid x_N(t_N)\right]_{\lambda_N}}$$

Each fraction in the above equation is the rate between the forward and backward transitions between two states under the same control parameter. If the system is Markovian and therefore independent from its history, this ratio of probabilities will be the same as for an equilibrium state. In other words, if the particle is known to be at a certain position at a certain time, it is not important whether it has been in equilibrium or not for a Markovian system. Therefore, each fraction in the above expression can be replaced by the energy difference between the initial and final energies of the particle according to Eq. (2.11):

$$\frac{P_{\mathrm{F}}(X)}{P_{\mathrm{R}}(\tilde{X})} = \underbrace{\frac{p\left[x_1(t_1) \mid x_0(t_0)\right]_{\lambda_1}}{p\left[x_0(t_0) \mid x_1(t_1)\right]_{\lambda_1}}}_{\exp(-\beta Q_1)} \cdots \underbrace{\frac{p\left[x_n(t_n) \mid x_{n-1}(t_{n-1})\right]_{\lambda_n}}{p\left[x_n(t_n) \mid x_{n-1}(t_{n-1})\right]_{\lambda_n}}}_{\exp(-\beta Q_n)} \cdots \underbrace{\frac{p\left[x_N(t_N) \mid x_{N-1}(t_{N-1})\right]_{\lambda_N}}{p\left[x_{N-1}(t_{N-1}) \mid x_N(t_N)\right]_{\lambda_N}}}_{\exp(-\beta Q_N)} \tag{3.13}$$

$$\frac{P_{\mathrm{F}}(X)}{P_{\mathrm{R}}(\tilde{X})} = \exp\left[-\beta(Q_1 + Q_2 + Q_3 + ... + Q_N)\right] \tag{3.14}$$

which leads to Eq. (3.3):

$$\frac{P_F(X(t), \lambda(t) \mid x(t_0) = x_0)}{P_R(\tilde{X}(t), \tilde{\lambda}(t) \mid x(t_0) = x_N)} = e^{-\beta Q}$$

where $Q = Q_1 + Q_2 + Q_3 + ... + Q_N$ is the total heat exchange from the thermal bath to the particle during the forward protocol. Note that this equation holds if the initial position is set to x_0 in the forward and x_N in the backward process. If the systems are initially thermalized, we have to multiply the probability of the initial position of the required trajectory:

$$\frac{P_F(X(t), \lambda(t))}{P_R(\tilde{X}(t), \tilde{\lambda}(t))} = e^{-\beta Q} \frac{p_{eq}(x_0, \lambda_0)}{p_{eq}(x_N, \lambda_{N+1})} = e^{-\beta Q} \frac{\exp(-\beta(U(x_0, \lambda_0) - F_i)}{\exp(-\beta(U(x_N, \lambda_{N+1}) - F_f)} \tag{3.15}$$

which leads to:

$$\frac{P_F(X(t),\lambda(t))}{P_R(\tilde{X}(t),\tilde{\lambda}(t))} = e^{\beta(\Delta U - Q - \Delta F)} = e^{\beta(W-\Delta F)} \tag{3.16}$$

This means that all the trajectories that yield the same work in a non-equilibrium process are equally likely to be reversed under time-reversed protocol if the system is initially thermalized. Therefore, we have derived Eq. (3.4):

$$\frac{P_F(+W)}{P_R(-W)} = e^{\beta(W-\Delta F)} \tag{3.17}$$

This equation can be easily tested since work can easily be quantified along stochastic trajectories as explained in the previous chapter. I will provide a numerical example of how Crooks fluctuation theorem can be seen in an arbitrary non-equilibrium process.

Example 3.1: Crooks fluctuation theorem in an arbitrary process

Here, I simulate a Brownian particle, which is held in a time-dependent potential:

$$U(x,\lambda(t)) = \frac{Kx^4}{4}\lambda(t) + \frac{kx^2}{2}\left(1-2\lambda(t)\right) \tag{3.18}$$

Initially I keep $\lambda = 1$ fixed for 2 seconds in order for the particle to thermalize in the trap. Then I change $\lambda(t)$ from 1 to 0 within a duration τ in the forward process, which corresponds to a transition from a double well into a harmonic potential, shown in Fig. 3.2(a). I calculate the work done along this forward trajectories over many realizations and obtain work distribution $P_F(W)$ for $\tau = 200$ ms (red solid line), $\tau = 50$ ms (blue solid line) and $\tau = 20$ ms (magenta solid line), as shown in Fig. 3.2(c). After that, I do the same operation for the reverse protocol: I keep $\lambda = 0$ for 2 seconds for relaxation and change $\lambda(t)$ from 0 to 1 within the same τ values, as shown in Fig. 3.2(b). Then I find the distribution of the work done on the particle along the time reversed protocol $P_R(-W)$ for $\tau = 200$ ms (red dashed line), $\tau = 50$ ms (blue dashed line) and $\tau = 20$ ms (magenta dashed line); as shown in Fig. 3.2(c). The rates of applied work in the forward processes and the extracted work in the backward processes are computed and displayed in Fig. 3.2(d), which verifies Eq. (3.4).

This example shows that, as we drive systems between equilibrium positions faster, the process becomes more and more irreversible as you can see from splitting work distributions along forward and time-reversed realizations for small driving times. Nevertheless, the Crooks fluctuation theorem holds true no matter how fast or slow we change the parameters, as shown in Fig. 3.2(d).

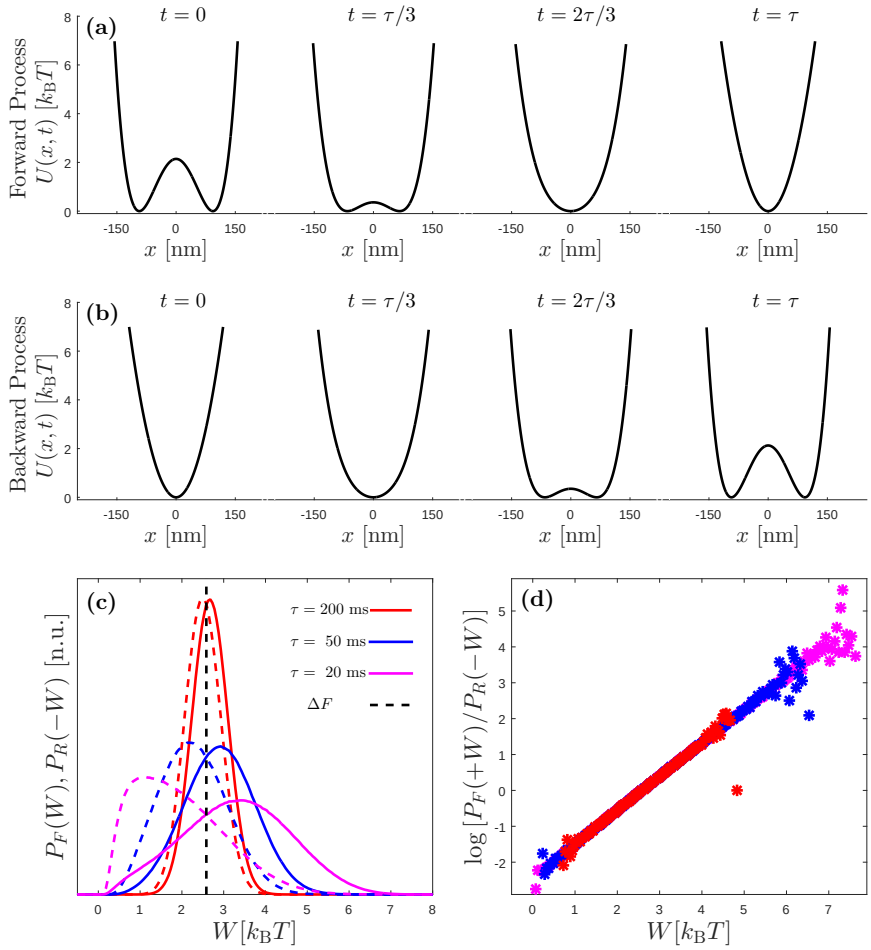

Figure 3.2: **Verification of Crooks fluctuation theorem in an arbitrary process.** **(a)** The forward protocol is demonstrated. Initially the particle is held in a bistable potential and the potential changes into a harmonic potential within time τ. **(b)** The backward protocol is demonstrated; this is the opposite of the protocol shown in (a) as explained in the example 3.1. **(c)** Resulting work distributions in the forward (solid lines) and backward (dashed lines) processes for different driving time τ. Note that no matter how fast we operate the process, $P_F(+W)$ and $P_R(-W)$ are equal at the value of the change in free energy ΔF (black dashed line). **(d)** The rate of probabilities of the applied work in the forward protocol and extracted work in the backward protocol. For various durations of the protocol, Eq. (3.4) is verified. Work distributions are obtained by repeating the protocols 10 million times. Matlab code that produced these results is provided in appendix B.

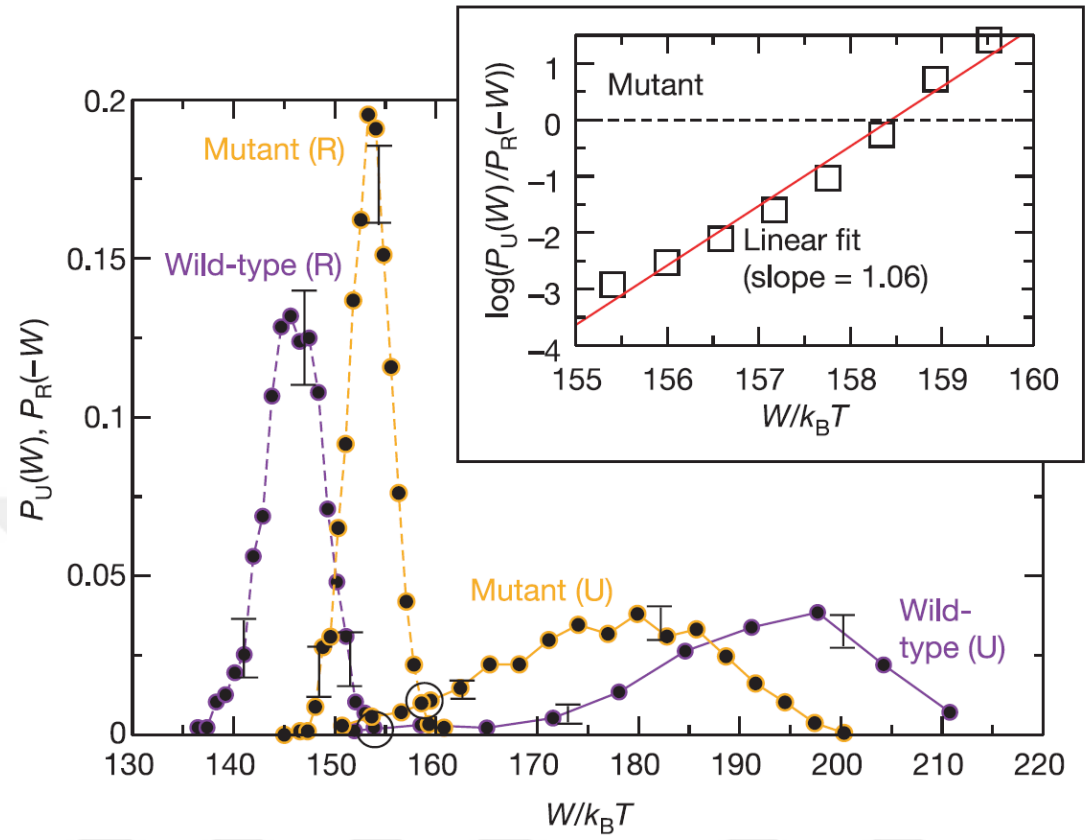

Figure 3.3: **Experimental verification of Crooks fluctuation theorem.** The wild-type and mutant single RNA molecules are attached to a bigger colloidal particle and stretched by optical tweezers. By repeating the forward protocol (Unfolding, continuous lines) and backward protocol (refolding, dashed lines) many times, histogram of work values obtained. Wild type pulling experiments were repeated 900 times (purple) and mutant type pulling experiments were repeated 1200 times (orange). Black circles mark the work values where $P_U = P_R$. The error bars represent the reproducibility of the data via repetition of the experiment. Inset: The linear behaviour of . Adapted from P_U/P_R with respect to W, in agreement with Eq. eq:WFT. Adapted from [8].

The first experimental verification of Crooks fluctuation theorem was performed by RNA stretching experiment with optical tweezers [8]. They verified Eq. (3.4) by measuring the work applied on a colloidal particle that is attached to an RNA molecule. They measured work values both in unfolding (forward) and refolding (backward) processes. The resulting work distribution did not only verify Crooks fluctuation theorem, but also enabled the authors to identify the free energy difference between folded and unfolded RNA molecules. Also, from

the work distribution they were able to differentiate between wild type and mutant RNAs. These results are shown in Fig. (3.3), which is adapted from the same work [8].

3.2 Jarzynski equality

In this section, I will give one of several different proofs [35] of Jarzynski equality, which will be followed by a numerical illustration. Then I will give a short discussion about the importance and the impact of this relation. Finally, I will conclude by highlighting an experimental verification of this equation.

Assume that we are looking for the following average in a non-equilibrium process:

$$\langle \exp\left(-\beta W\right)\rangle = \int \exp\left(-\beta W\right) P_F(W) dW$$

Here, $P_F(W)$ is the probability distribution of applying W amount of work along the forward non-equilibrium process. Substituting $P_F(W)$ from Eq. (3.4) immediately solves the RHS of the above equation:

$$\langle \exp\left(-\beta W\right)\rangle = \int \exp\left(-\beta W\right) P_R(-W) \exp\left[\beta(W-\Delta F)\right] dW \tag{3.19}$$

$$= \int \exp\left(-\beta \Delta F\right) P_R(-W) dW \tag{3.20}$$

where $\exp\left(-\beta\Delta F\right)$ is a constant and can be taken outside of the integral. The rest is just the sum over all probabilities of the work applied during backward process, which is trivially 1 according to normalization. Therefore, we have obtained the Jarzynski equality:

$$\langle \exp\left(-\beta W\right)\rangle = \exp\left(-\beta \Delta F\right) \tag{3.21}$$

Please note that this relation is alvo valid only if the system is initially at thermal equilibrium. Hatano and Sasa [50] formulated a generalized version of

Jarzynski equality when a system is not initially in an equilibrium state but in a non-equilibrium steady state. This relation is very useful as it relates the free energy differences between two equilibrium states if the work distribution is known. One important property is Eq. (3.1) holds no matter how fast or irreversible we perform the driving of the potential.

Another important property of the Jarzynski equality is that one can reconstruct the free energy landscape of all the intermediate states during a non-equilibrium process [51, 55]. Assume that the process starts at $t = t_0$ from the control parameter λ_0 and ends at $t = t_f$ with λ_f. At any internediate time t, we can write:

$$\langle \exp\left(-\beta W(t)\right)\rangle = \exp\left(-\beta \Delta F_{\lambda(t),\lambda_0}\right) \tag{3.22}$$

Eq. (3.22) permits one to find out the free energy difference between the initial state and any of the intermediate states. I will show a numerical example depicting how Eq. (3.1) and Eq. (3.22) work in a time dependent harmonic trap.

Example 3.2: Jarzynski relation and free energy reconstruction
Consider that we have a Brownian particle in a thermal bath that is kept in a time dependent harmonic potential:

$$U(x, \lambda(t)) = \frac{1}{2}k[3 + 2sin(\omega t)]x^2 \tag{3.23}$$

where the trap stiffness changes in a sinusoidal manner. This process is shown in Fig. 3.4(a). The applied work on the particle is averaged over many realizations of the same protocol. The average applied work on the particle as a function of time is shown in Fig. 3.4(b), which is in agreement with the second law. I also verify Eq. (3.1) and Eq. (3.22) by taking the exponential average of the work applied as a function of time and comparing this to the Boltzmann weighted change in free energy, as shown in Fig. 3.4(c).
In conclusion, if the work distribution is known as a function of time for a non-equilibrium process, one can identify free energy differences between initial and final states employing Eq. (3.1), or can reconstruct the whole free energy landscape of the process as a function of intermediate states employing Eq. (3.22).

Jarzynski equality was first verified in 2002 [7] using an RNA stretching experiment. Such an operation can be performed by linking RNA to a greater colloidal particle and employing optical tweezers [65, 42] to stretch RNA and photonic force microscopy to analyze forces [66]. Also, this relation has been tested for single molecules [59, 9, 58, 8], mechanical oscillators [10], electronic systems [64] and colloidal particles in non-harmonic potentials [11]. Also, it is tested and verified for quantum systems, where work measurements were done on a trapped ion system that was thermalized by phonons [62]. As an example, I adapt the results from a single molecule strecthing experiment [59], where the authors stretched a titin I27 molecule at different speeds and succesfully recovered the same free energy profile. These results are shown in Fig. 3.5.

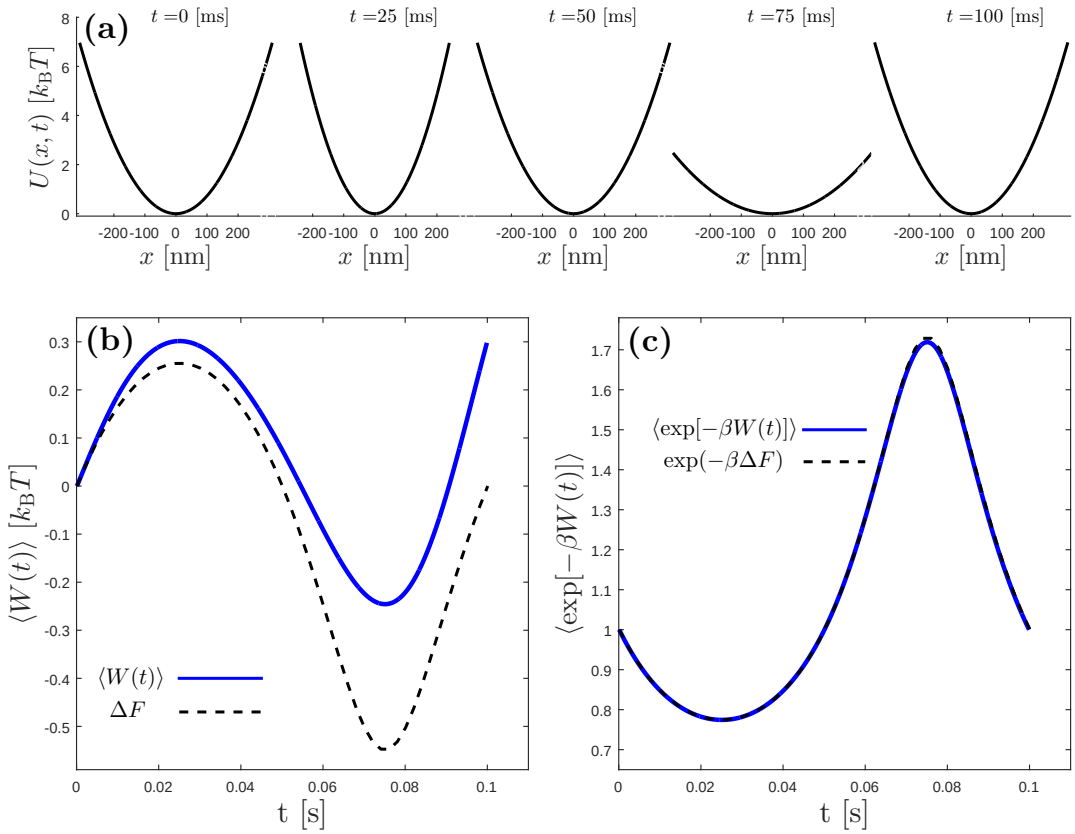

Figure 3.4: **Illustration of Jarzynski equality in a time-dependent harmonic trap. (a)** The protocol is sketched. First, the stifness is increased, then decreased and then finally taken back to its initial vaue. This protocol is quantitatively explained in example 3.2. **(b)** The average work applied as a function of time during the process described in (a). Note that in average, one applies greater work than the change in free energy in an irreversible process. **(c)** Verification of Jarzynski equality. The Boltzmann weighted exponential average of the work applied follows exactly the Boltzmann weighted exponential of the change in free energy. The work values are averages over 100000 realizations of the same protocol. The Matlab code that produced these results are provided in appendix B.

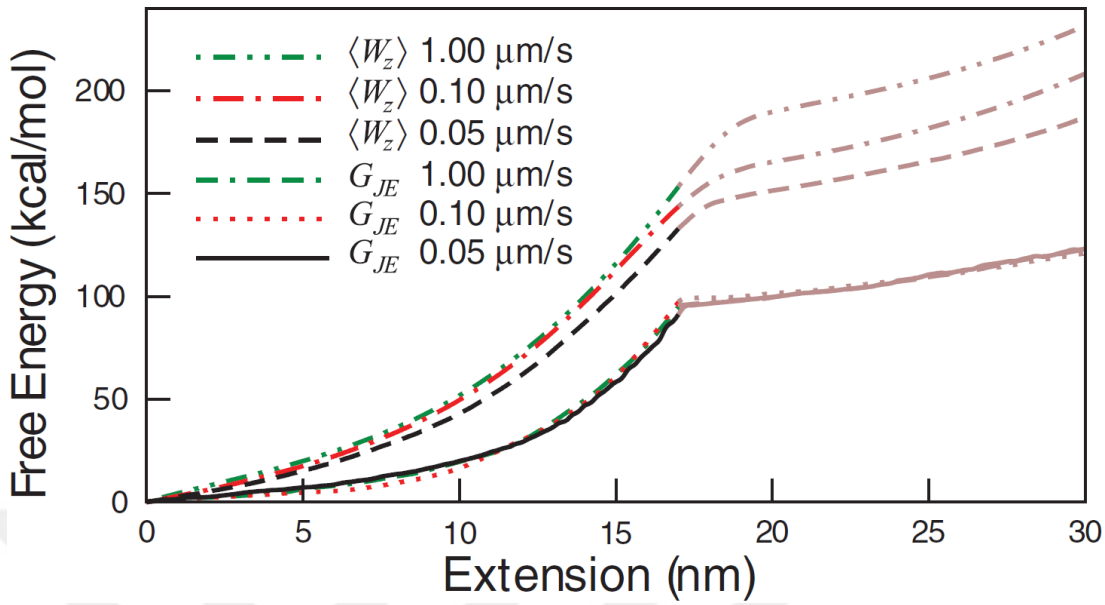

Figure 3.5: **Experimental free energy reconstruction using Jarzynski equality** Estimating free energy profile using Jarzynski estimator (Eq. (3.22)). Single molecule stretching experiments were carried out on a titin I27 at different pulling velocities. Note that as the pulling velocity increases, the process is more irreversible and therefore the average work applied is also increases. However, the estimated free energy profiles with Jarzynski estimator always gives the same free energy profile no matter how fast the molecule is pulled. Adapted from [59]

3.3 Integral Fluctuation Theorem

Here, I will demonstrate the integral fluctuation theorem [6], which concerns the heat exchange between a system and the heat bath rather than the work applied. I will begin with giving an analytical derivation.

Let us recall Eq. (3.3):

$$\underbrace{\frac{\overbrace{P_F(X(t),\lambda(t)\mid x(t_0)=x_0)}^{P_F(X(t))/p(x_0,\lambda_0)}}{\underbrace{P_R(\tilde{X}(t),\tilde{\lambda}(t)\mid x(t_0)=x_f)}_{P_R(\tilde{X}(t))/p(x_f,\lambda_f)}}}_{} = e^{-\beta Q}$$

$$\frac{P_F(X(t))}{P_R(\tilde{X}(t))} = e^{-\beta Q}\frac{p(x_0,\lambda_0)}{p(x_f,\lambda_f)} = \exp\left[-\left(\beta Q - \log\frac{p(x_0,\lambda_0)}{p(x_f,\lambda_f)}\right)\right]$$

$$P_F(X(t))\exp\left[\beta Q - \log\frac{p(x_0,\lambda_0)}{p(x_f,\lambda_f)}\right] = P_R(\tilde{X}(t)) \tag{3.24}$$

We can multiply both sides with dX and integrate:

$$\int \exp\left[\beta Q - \log\frac{p(x_0,\lambda_0)}{p(x_f,\lambda_f)}\right] P_F(X(t))dX = \int P_R(\tilde{X}(t))dX$$

note that $dX = d\tilde{X}$ because $\tilde{X}$ is the reversed trajectory of X. Therefore, we have an average over all possible trajectories on the left hand side, and a probability summation on the right hand side:

$$\int \exp\left[\beta Q - \frac{p(x_0,\lambda_0)}{p(x_f,\lambda_f)}\right] P_F(X(t))dX = \underbrace{\int P_R(\tilde{X}(t))d\tilde{X}}_{1}$$

$$\left\langle \exp\left[\beta Q - \frac{p(x_0,\lambda_0)}{p(x_f,\lambda_f)}\right]\right\rangle = 1 \tag{3.25}$$

Note that this relation does not require an initial Boltzmann distribution, the system is not required to have reached an equilibrium state before the driving process. Under certain assumptions, this equality may simplify to the Hatano-Sasa relation or Jarzynski equality, but this is a universal equality that one can employ without any assumptions about the initial probability conditions [57, 34].

Chapter 4

A non-Markovian environment: Active matter

So far, I have discussed the stationary distributions and non-equilibrium relations of thermal systems, which are Markovian and therefore, microscopically reversible. Active systems, however, are subject to active noise that may arise from biological media or artificial activity like self-propelled particles. Thus, these systems are intrinsically out of equilibrium and presumed to be examined only in the framework of non-equilibrium physics [67, 68, 32, 69, 70]. There have been several studies in which scientists have discussed to what extend statistical physics can be applied to such active systems [12, 13]. In this section, I will give an overview of how active systems can be characterised by the properties of their activity and under which conditions their activity could be mapped to thermal systems with enhanced effective temperatures.

An active Brownian particle is able to self-propel [71]. Most common agents that come across in nature that could be categorized as an active Brownian particles are swimming microorganisms like *Escherichia coli* [72]. Some microorganisms in nature may exhibit run-and-tumble motion, which corresponds to swimming in a certain direction for a while and stopping for a while to reorient itself [73], which have similar statistical behaviour and difusion characteristics to

smooth swimmers [74]. Such an activity can also be realized with an artifical swimmer which creates asymmetry around its viscinity to induce self-propulsion [75]. Such a mechanism can be realized with various techniques such as chemical asymmetry [76, 77, 14], thermophoresis [78] or critical demixing [79]. A self-propelling particle propels itself with a constant force which results in the following set of Langevin equations:

$$\dot{x} = V\cos(\phi)\sqrt{2D_T}W_x(t) \tag{4.1}$$

$$\dot{y} = V\sin(\phi)\sqrt{2D_T}W_y(t) \tag{4.2}$$

$$\dot{\phi} = \sqrt{2D_R}W_\phi(t) \tag{4.3}$$

where ϕ represents the orientation of the self-propelled particle, which is subject to rotational diffusion. Here, W_x, W_y and W_ϕ are white noises with zero mean and unitary variance. The mean square displacement of such a swimmer in 2 dimensions can be analytically derived as [80, 14]:

$$\mathrm{MSD}(t) = [4D_T + V^2\tau_R]t + \frac{V^2\tau_R^2}{2}\left[e^{\frac{-2t}{\tau_R}} - 1\right] \tag{4.4}$$

while τ_R represents the characteristic timescale of particles rotational motion. This leads to 3 different phenomenon to be observed for an active particle at different timescales:

1. Standart diffusive regime, when $t << \tau_R$. The resulting MSD will take the form

   $$\mathrm{MSD}(t) = 4D_T t$$

   Here, the slope of MSD-t graph will be 1 as it performs regular diffusion.

2. Superdiffusive regime, when $t \approx \tau_R$. At this timescale, one would need the Eq. (4.4) to explain fully the dynamics. In this regime, the slope of MSD-t graph will be between 1 and 2.

3. Enchanced diffusion regime. In the limit when $t >> \tau_R$. Here, MSD of the particle will be given as:

   $$\mathrm{MSD}(t) = (4D_T + V^2\tau_R)t$$

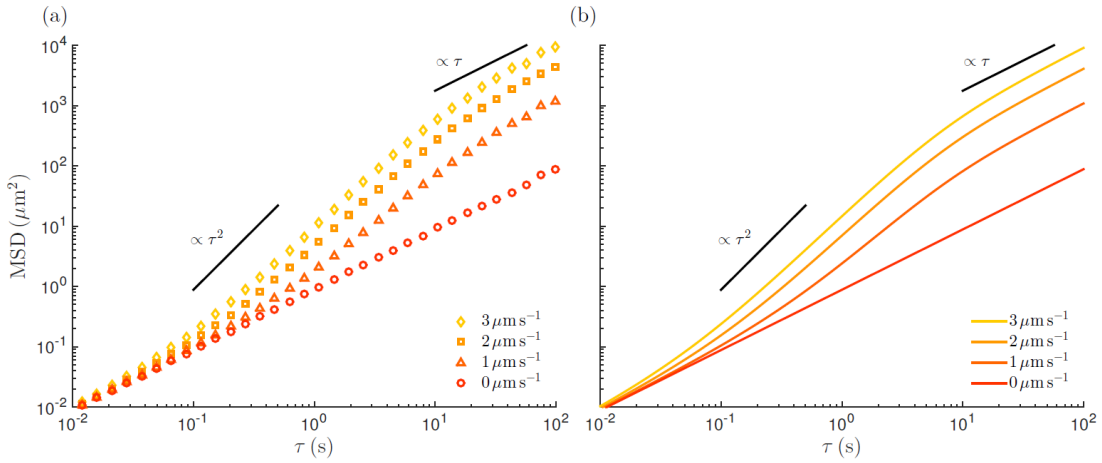

Figure 4.1: **Mean square displacement (MSD) of active Brownian particles and effective diffusion coefficients.** (a) Numerically calculated and (b) theoretical MSD for active Brownian particles with velocity $V = 0$ μm s^{-1} (circles), $V = 1$ μm s^{-1} (triangles), $V = 2$ μm s^{-1} (squares) and $V = 3$ μm s^{-1} (diamonds). For passive Brownian particles ($V = 0$ μm s^{-1}, circles) the motion is always diffusive, while for active Brownian particles the motion is diffusive with diffusion constant D_T at very short timescales, ($\tau << \tau_R$), ballistic at intermediate timescales ($\tau \approx \tau_R$), and again diffusive but with an enhanced diffusion constant at long time scales ($\tau >> \tau_R$). Adapted from [13].

Here, the slope of MSD-t graph will go back to 1, and diffusion properties of the system can be represented with an effective temperature $T_{\text{eff}} = T + \frac{\gamma V^2 \tau_R}{4k_B}$

These 3 regimes are demonstrated nicely in a recent review paper, which is shown in Fig. 4.1. Please note that these categorization of timescales ignores the inertial timescales when $t \approx m/\gamma$, where m/γ is the momentum relaxation time of the Brownian particle. For such ultra short timescales, particle exhibits ballistic motion and therefore, the slope of MSD-t curve is expected to be 2. However, for typical soft matter experiments, this number corresponds to fraction of a microsecond, which is not accesible for standart position measurement techniques like digital video microscopy or interferometry [42]. Nevertheless, this regime has been explored experimentally by using high-bandwidth quadrant photodiodes [81, 82, 83].

Passive particles can also exhibit similar diffusive behaviour when they are

immersed in an environment in which there are plenty of active particles, e.g. motile bacteria which is called an active bath [84, 85]. All these systems are called non-Markovian as in short timescales when t and τ_R are comparable to each other as the particle's velocity becomes correlated, which results in the violation of equilibrium conditions and time reversal symmetry. Under such conditions, lots of interesting non-equilibrium phenomenon are observed like crowd control [17], directed transport [86, 18, 87, 88, 89], cluster formation [90, 91, 92] and energy harvesting from a single bath [93, 94]; all of which are not possible to observe in a Markovian environment.

Chapter 5

Equilibrium or non-equilibrium? Results on experimental investigation of stationary distributions

Already at the beginning of the 20^{th} century, classical thermodynamics provided a comprehensive understanding of the equilibrium behavior of macroscopic systems in contact with thermal reservoirs and deterministic relations between their thermodynamic quantities [95]. Instead, it has only been during the last few decades that the thermodynamics of non-equilibrium systems and active matter has become the subject of intense research [35, 34, 12]. This interest is motivated by the need of exploring the physics of microscopic systems, where thermal fluctuations play a crucial role and introduce stochasticity [3, 96], and of living matter, which is intrinsically far from equilibrium [97, 13]. On the one hand, for microscopic systems thermal fluctuations become essential because of the limited number of degrees of freedom and can generate outcomes that are forbidden in macroscopic systems. For example, the presence of thermal fluctuations allows the violation of the second law for single realizations of a process, even though the second law

still holds on average [3, 96, 98, 99]. A major advance in stochastic thermodynamics has been the realization that, instead of just averaging the fluctuations out, it is possible to make use of the information they contain in order to recover equilibrium information even from non-equilibrium measurements using, e.g., the Jarzynski equality and Crooks fluctuation theorem [4, 57, 49, 5, 57, 35, 34]. These relations have recently been tested and verified experimentally for various systems that are coupled to thermal baths [7, 8, 58, 59, 11, 62, 9, 10, 64]. On the other hand, many systems, such as living matter, are intrinsically far from equilibrium. For example, biomolecules within the cell are coupled with an active bath due to the presence of molecular motors within the cytoplasm, which leads to striking and largely not yet understood phenomena such as the emergence of anomalous diffusion [97]. Also, protein folding might be facilitated by the presence of active fluctuations [100] and active matter dynamics could play a central role in several biological functions [101, 102, 103]. Until now, the experimental study of all these systems has been limited [13].

Here, we present a series of experiments with an optically trapped Brownian particle coupled to an active bath. First, we show that in an active bath the statistical properties of a particle held in a potential do not generally follow the Boltzmann statistics because of the correlated noise introduced by the active bath: as the characteristic scale of the optical trap becomes comparable to the correlation length introducted by the active noise, we observe a transition between a regime that can be described with Boltzmann statistics (albeit at a higher effective temperature) to a regime that follows non-Boltzmann statistics. Then, we also show that a major consequence of this fact is that non-equilibrium relations, such as Crooks fluctuation theorem [5], Jarzynski equality [4], and the integral fluctuation theorem [57], cannot be applied in active baths according to their classical formulation; we show nevertheless that they can be recovered by introducing an effective potential. Our findings pose some significant limitations to the possibility of applying non-equilibrium fluctuation-dissipation relations to active matter systems, including living matter, and point to the need for alternative approaches that explicitly model the presence of non-thermal fluctuations, such as the use of effective potentials that play the same role as thermodynamic

potentials in passive baths.

5.1 Non-Boltzmann stationary distribution in active baths

The motion of a Brownian particle immersed in a liquid at temperature T is described by the overdamped Langevin equation:

$$\frac{dx}{dt} = -\frac{1}{\gamma}\frac{dV(x)}{dx}dt + \eta_{\mathrm{p}} \,, \tag{5.1}$$

where x is the particle position, γ is the particle friction coefficient, $V(x)$ is the potential, η_{p} represents the (white) thermal noise characterized by $\langle \eta_{\mathrm{p}}(t+\tau)\eta_{\mathrm{p}}(t)\rangle = 2D_{\mathrm{p}}\delta(\tau)$, and D_{p} is the translational diffusion coefficient, which importantly is related to γ by the fluctuation-dissipation relation $D_{\mathrm{p}}\gamma = k_{\mathrm{B}}T$. The corresponding position (equilibrium) distribution follows Boltzmann distribution:

$$p(x) = Z^{-1}\exp\left(-\frac{V(x)}{k_{\mathrm{B}}T}\right) \,, \tag{5.2}$$

where $Z = \int_{-\infty}^{+\infty}\exp(-\beta V(x))dx$ is the partition function.

Experimentally we employ a spherical Brownian microparticle (polystyrene, diameter $2R = 4.06 \pm 0.20\,\mu$m) in a watery solution trapped by an optical trap generated by focusing a laser beam (wavelength $\lambda = 976\,$nm) with a high-numerical-aperture objective (oil-immersion, $\times 100$, NA = 1.30) [42]. The optical potential is harmonic:

$$V_{\mathrm{ot}}(x) = \frac{1}{2}kx^2 \tag{5.3}$$

with stiffness k, which is proportional to the laser intensity and can, therefore, be adjusted by using some neutral density filters along the laser beam path. The expected Boltzmann position distribution (Eq. 5.2) is Gaussian:

$$p_{\mathrm{ot}}(x) = Z_{\mathrm{ot}}^{-1}\exp\left(-\frac{kx^2}{2k_{\mathrm{B}}T}\right) \,, \tag{5.4}$$

where $Z_{\mathrm{ot}} = \sqrt{\frac{2\pi k_{\mathrm{B}}T}{k}}$ is the normalization prefactor. The particle position is monitored by digital video microscopy (using the radial symmetry algorithm [104])

with a spatial resolution of 5 nm. The results are plotted by the blue symbols in Figs. 5.1a, 5.1b, and 5.1c for $k = 0.42\,\mathrm{fN\,nm^{-1}}$, $3.6\,\mathrm{fN\,nm^{-1}}$, and $22\,\mathrm{fN\,nm^{-1}}$, respectively. As expected from Eq. (5.4), the resulting distributions are Gaussians with variance $\propto k^{-1}$ (dashed blue lines in Figs. 5.1a, 5.1b, and 5.1c) and are in very good agreement with the experimental data. The characteristic timescale with which the particle is attracted towards the center of the harmonic trapping potential is given by $\tau_{\mathrm{ot}} = \gamma/k$ [42]; we obtain $\tau_{\mathrm{ot}} = 190\,\mathrm{ms}$, 22 ms, and 4 ms for the data reported in Figs. 5.1a, 5.1b, and 5.1c, respectively.

We now consider a Brownian particle in an active bath. We realize the active bath by adding motile bacteria to the watery solution where the particle is immersed [85, 17] (inset in Fig. 5.2a): the bacteria behave as active particles and exert non-thermal forces on our probe particle so that it experiences non-thermal fluctuations and features a qualitatively different behavior from that of a Brownian particle in a thermal bath. We do not observe any accumulation of bacteria around the focal spot due to the optical force; this can be understood because the optical forces acting on the bacteria (which have a small polarizability due to their small size and low refractive index mismatch) are much weaker than self-propulsion forces. The Langevin equation that describes this system is

$$\frac{dx}{dt} = -\frac{1}{\gamma}\frac{dV(x)}{dx}dt + \eta_{\mathrm{p}} + \eta_{\mathrm{a}}\ , \tag{5.5}$$

where η_{a} represents the fluctuations due to the presence of the active bath. This is an additional source of noise that must be added to Eq. (5.1) in order to describe the dynamics of the particle; unlike thermal fluctuations, these fluctuations are exponentially correlated over time so that $\langle \eta_{\mathrm{a}}(t+\tau)\eta_{\mathrm{a}}(t)\rangle = \frac{L_{\mathrm{a}}^2}{\tau_{\mathrm{a}}^2}\exp(-\tau/\tau_{\mathrm{a}})$, where τ_{a} is the persistence time of the bacterial forces acting on the particle associated with a persistence length L_{a}, i.e., a characteristic distance along which the bacteria drag (in average) the particle [85, 105, 106, 17, 107]. It is important to remark at this point that the introduction of Eq. (5.5) does not entail that the distribution of η_{a} is Gaussian. A characteristic trajectory of a Brownian particle in an active bath ($V(x) \equiv 0$) is shown by the red line in Fig. 5.2a. The mean square displacement (MSD) of this particle is shown by the symbols in Fig. 5.2b. This MSD features a transition from a superdiffusive regime at short time scales to enhanced diffusion at long time scales. Fitting this MSD to its theoretical

formula [108], i.e.,

$$\mathrm{MSD}(t) = 2D_{\mathrm{p}}t + \frac{L_{\mathrm{a}}^2}{\tau_{\mathrm{a}}}\left[t - \tau_{\mathrm{a}}\left(1 - e^{-\frac{t}{\tau_{\mathrm{a}}}}\right)\right] \tag{5.6}$$

permits us to obtain the value of $\tau_{\mathrm{a}} = 140\,\mathrm{ms}$ and $L_{\mathrm{a}} = 296\,\mathrm{nm}$. Importantly, the presence of the active noise introduces a memory in the fluctuation forces that is not matched by a corresponding memory in the friction term; this is a signature that the fluctuations of the probe particle are out of equilibrium.

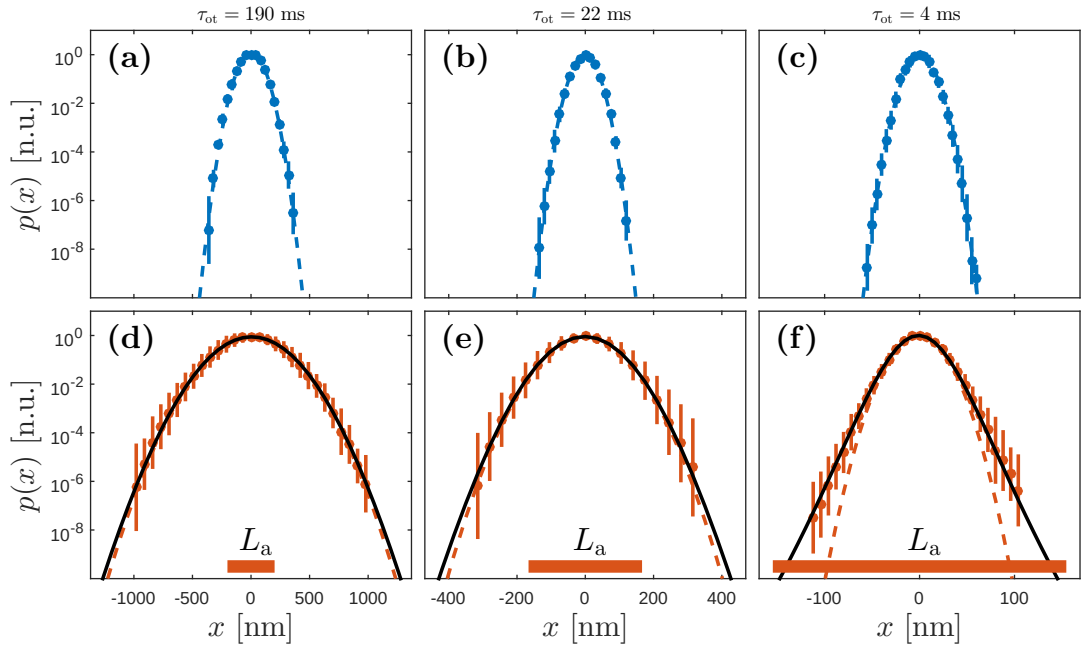

Figure 5.1: **Emergence of non-Boltzmann position distributions in active baths.** (a-c) Measured position distributions (blue symbols) and corresponding Gaussian distributions (dashed blue lines) for a Brownian particle in a thermal bath confined in a harmonic trapping potential with trapping stiffness (a) $k = 0.42\,\mathrm{fN\,nm^{-1}}$, (b) $k = 3.6\,\mathrm{fN\,nm^{-1}}$, and (c) $k = 22\,\mathrm{fN\,nm^{-1}}$. As k is increased, the particle becomes more confined, but the distribution remains Gaussian. Note the different scales for the position axes. (d-f) Measured position distributions (red symbols) and best Gaussian fits (red dashed lines) for a Brownian particle in an active bath in a harmonic trapping potential with trapping stiffness (d) $k = 0.42\,\mathrm{fN\,nm^{-1}}$, (e) $k = 3.6\,\mathrm{fN\,nm^{-1}}$, and (f) $k = 22\,\mathrm{fN\,nm^{-1}}$. As k is increased, the particle gets confined within a lengthscale comparable to the persistence length in the active bath (L_a, red bars in (d), (e), and (f)); consequently, the distribution deviates from a Gaussian and can be fitted with a heavy-tailed q-Gaussian distribution (solid black line) with $q = 1.013$, 1.023, and 1.142 for (d), (e), and (f) respectively ($q = 0.997$, 1.000, and 1.001 for (a), (b), and (c), compatibly with a Gaussian profile). The data are obtained from 200-s long trajectories acquired at about 400 fps; the error bars are obtained by repeating the measurements six times.

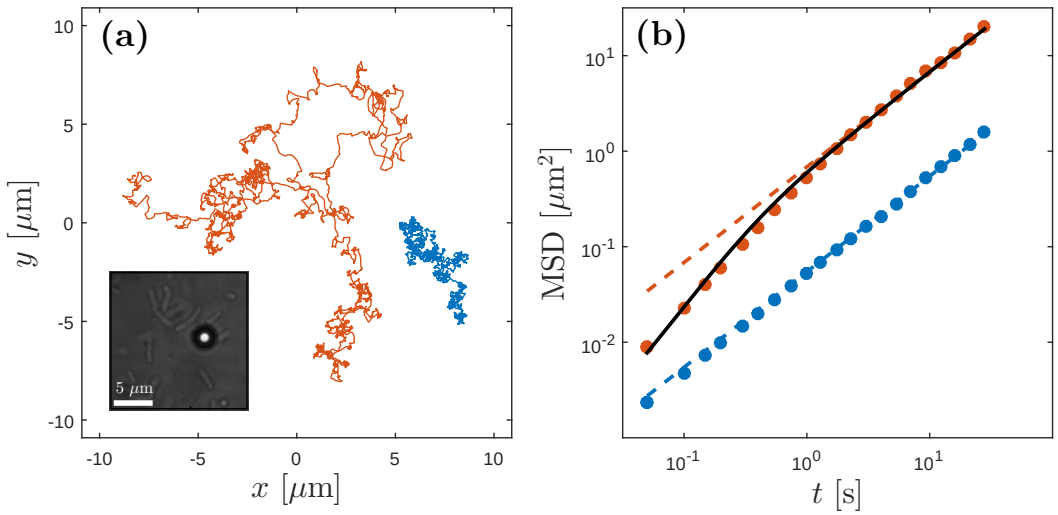

Figure 5.2: **Particle in an active bath.** (a) Sample trajectories of a microscopic particle (polystyrene, diameter $2R = 4.06 \pm 0.20\,\mu$m) in an active (bacterial) bath (red line) and in a thermal bath (blue line). The trajectories are extracted from a 150-s video sampled at 20 fps. Inset: A sample frame from the acquired video in the active bath; the bright spot corresponds to the particle, while the elongated lighter objects are the bacteria. (b) The mean square displacement (MSD) of the particle in the active bath along one axis (red symbols) features a transition from a superdiffusive regime at short time scales to enhanced diffusion at long time scales, differently from the MSD of the particle in the thermal bath (blue symbols).

We will now add the optical trap. In a weak trap ($k = 0.42\,\mathrm{fN\,nm^{-1}}$, $\tau_{\mathrm{ot}} = 190\,\mathrm{ms}$), the particle position distribution remains Gaussian, as shown by the experimental data (red symbols) in Fig. 5.1d. Since the persistence length associated with the active bath (L_{a}, red bar in Fig. 5.1d) is much shorter than the characteristic dimension of the trap, the motion of the particle can be described as a standard Brownian motion in a harmonic potential, but at a higher effective temperature $T_{\mathrm{eff}} = 2300\,\mathrm{K}$, in agreement with previous works [108]. Thus, these data can be fitted to a Gaussian (dashed red line), albeit with a variance larger than in the case of the thermal bath (Fig. 5.1a), despite the trap stiffness being

the same:

$$p_{\mathrm{ot,eff}}(x) = Z_{\mathrm{ot,eff}}^{-1} \exp\left(-\frac{kx^2}{2k_{\mathrm{B}}T_{\mathrm{eff}}}\right) . \tag{5.7}$$

where $Z_{\mathrm{ot,eff}} = \sqrt{\frac{2\pi k_{\mathrm{B}}T_{\mathrm{eff}}}{k}}$ is the normalization prefactor.

However, as the trap stiffness increases, L_{a} becomes comparable to the characteristic dimension of the trap and the experimental position probability distribution (red symbols in Figs. 5.1e and 5.1f) become non-Gaussian, as can be seen by comparing these data with the best Gaussian fits (red dashed lines). This becomes particularly evident when considering the tails of the distribution, which are clearly heavier than expected from the Gaussian distributions. Importantly, these distributions are non-Boltzmann, which implies that the case of a particle in an active bath is qualitatively different from the case of a particle in a thermal bath. In fact, it is not possible to recover this probability distribution by altering the effective temperature of the system, as the position probability distribution associated with a Brownian particle in a harmonic potential is Gaussian at all temperatures. The alteration of the distribution is in fact due to the correlations introduced in the motion of the particle by the active bath, which lead to a non-Gaussian noise. Even though some works have demonstrated the possibility of having Boltzmann distribution at long length scales [108] and others have implicitly indicated the breakdown of Boltzmann statistics at short length scales [105, 17, 18], here we explicitly report a transition from Boltzmann regime where it is possible to adopt a description based on effective temperatures to a non-Boltzmann regime where system's deviation from a Boltzmann description is quantified.

The experimental probability distributions can be fitted using q-Gaussian distributions [109, 110], which are generalizations of the Gaussian distribution that depend on a parameter q:

$$p_q(x) = Z_q^{-1} \exp_q\left(-\frac{kx^2}{2k_{\mathrm{B}}T_{\mathrm{eff}}}\right) , \tag{5.8}$$

where Z_q is a normalization prefactor and $\exp_q(y) = [1 + (1-q)y]^{\frac{1}{1-q}}$. Importantly, q-Gaussian distributions are characterized by heavy tails for $1 < q < 3$ and converge to the Gaussian distribution for $q \to 1$. The use of a q-Gaussian

distribution permits us to quantify the deviation from a Gaussian distribution by using the fitting parameter q: the greater the deviation of q from 1, the heavier the tail of the distribution. While the position probability distribution of the optically trapped particle in the thermal bath is well-fitted by a Gaussian distribution at all stiffnesses ($q = 0.997$, 1.000, and 1.001 for 5.1a, 5.1b, and 5.1c), those in the active bath become more and more heavy-tailed as the trap stiffness increases, i.e. $q = 1.013$, 1.023, and 1.142 for 5.1d, 5.1e, and 5.1f, respectively.

We underline that this transition from a situation that can be described with Boltzmann statistics, albeit at a higher effective temperature, and a situation that cannot be described by Boltzmann statistics associated with the ratio between the characteristic scales of the trapping potential and the correlated active noise underlies several results connected with broken symmetries in active matter [111, 112, 17, 18, 105, 93, 113].

Chapter 6

Results on experimental investigation of non-equilibrium relations in active baths

Building on the results obtained in the previous section, we will now show that non-equilibrium relations cannot be applied in active baths according to their classical formulation. Furthermore, we will show that they can be recovered by introducing an effective potential. We will in particular focus on Crooks fluctuation theorem [5], Jarzynski equality [4], and the integral fluctuation theorem [57].

Let us consider a system driven from an initial to a final state, such that the equilibrium free energy difference between the two states is ΔF and the applied work is W. Crooks fluctuation theorem [5] relates the probabilities of applying opposite works under forward and backward (time-reversed) protocols when a system is driven arbitrarily out of equilibrium [5]:

$$\frac{P_{\mathrm{F}}(+\beta W)}{P_{\mathrm{R}}(-\beta W)} = e^{\beta(W-\Delta F)} \ , \tag{6.1}$$

where $\beta = (k_{\mathrm{B}}T)^{-1}$, $P_{\mathrm{F}}(+\beta W)$ is the probability of applying $+W$ work in a forward protocol, and $P_{\mathrm{R}}(-\beta W)$ is the probability of applying $-W$ work in the

reversed protocol. An important precondition for Crooks fluctuation theorem to be valid is that the system should initially be in a thermal equilibrium state and, therefore, have Boltzmann distribution; since this initial condition is violated in an active bath (see Figs. 5.1e and 5.1f), we do not expect this relation to be verified in an active bath. The Jarzynski equality [4] allows one to obtain the free-energy difference from an exponential average of the work associated with irreversible realizations of a thermodynamic process:

$$\left\langle e^{-\beta W_i} \right\rangle = e^{-\beta \Delta F} \ , \tag{6.2}$$

where W_i is the i^{th} realization of the same protocol and brackets indicate average over many realizations. Importantly, the initial (Boltzmann) equilibrium condition is needed also for Jarzynski equality. Finally, a generalization of these results is the integral fluctuation theorem [57]:

$$\left\langle \exp\left(\beta Q - \log \frac{p(x_0)}{\tilde{p}(\tilde{x}_0)} \right) \right\rangle = 1 \ , \tag{6.3}$$

where Q is the heat exchanged by the driven system with the surrounding environment, and $p(x_0)$ and $\tilde{p}(\tilde{x}_0)$ are the initial and final probability distributions calculated at initial and final external parameters, respectively.

Experimentally, we consider a Brownian microparticle (silica, diameter $2R = 4.23 \pm 0.20\,\mu$m) held by a harmonic trap generated by focusing a laser beam (wavelength $\lambda = 532\,$nm, power $2.1\,$mW) with a high-numerical-aperture objective (oil-immersion, $\times 100$, NA $= 1.30$) [42]. The optical trap position can be translated using a spatial light modulator. The particle position is monitored by digital video microscopy with a spatial resolution of $5\,$nm and a sampling frequency of 50 frames per second. The resulting trapping potential is

$$V_{\text{ot}}(x,t) = \frac{1}{2} k \left(x - \lambda(t) \right)^2 \ , \tag{6.4}$$

where x is the position of the particle, t is time, $k = 1.33 \pm 0.05\,\text{fN nm}^{-1}$ is the trap stiffness, and $\lambda(t)$ denotes the center of the harmonic potential, which acts as our external control parameter. In our protocol, $\lambda(t)$ is a square-wave function with amplitude A and period 2τ: first, the potential is centered at position 0 (dashed red line in Fig. 6.1a) for a time interval τ; then, it is shifted to position

$A = 90\,\mathrm{nm}$ (solid red line in Fig. 6.1a), where it remains for an additional time interval τ; finally, the potential is brought back to position 0 and the protocol is iterated. The free energy of the optically trapped particle is

$$F = -\frac{1}{\beta}\ln\left(Z_{\mathrm{ot}}\right) \ , \tag{6.5}$$

which depends only on k and, importantly, not on the trap center position. Thus, since in our protocol the stiffness is kept constant, the free energy difference between the initial and the final state is zero, i.e., $\Delta F = 0$. Furthermore, because of symmetry, the forward and backward protocols are identical, i.e., $P_{\mathrm{F}}(y) = P_{\mathrm{R}}(y)$. Therefore, for our experimental realization, Crooks fluctuation theorem (Eq. (6.1)) and Jarzynski equality (Eq. (6.2)) simplify to

$$\frac{P(+W)}{P(-W)} = e^{\beta W} \tag{6.6}$$

and

$$\left\langle e^{-\beta W_i} \right\rangle = 1 \ . \tag{6.7}$$

We repeated 5000 times the experimental protocol described above and recorded the particle trajectory. Let t_i be the time when the i-th potential switch occurs, the work W_i applied on a particle during a sudden change of the external potential is equal to the instantaneous change in potential energy (dashed black line in Fig. 6.1a); therefore,

$$W_i = V_{\mathrm{ot}}(x\left(t_i\right), t_i^+) - V_{\mathrm{ot}}\left(x\left(t_i\right), t_i^-\right), \tag{6.8}$$

where $V_{\mathrm{ot}}(x, t_i^+)$ and $V_{\mathrm{ot}}(x, t_i^-)$ are the potentials after and before the shift of the center, respectively. This quantity is shown in Fig. 6.1b as a function of the position of the particle at the switching time. Initially, we performed our experiments in a thermal bath. Using the experimental work distributions obtained by Eq. (6.8), we verified that the Crooks fluctuation theorem (Eq. (6.6)) and Jarzynski equality (Eq. (6.7)) are satisfied in a thermal bath. In order to verify the integral fluctuation theorem Eq. (6.3), we need to evaluate the heat Q. According to the standard definition of heat in stochastic thermodynamics [114], the infinitesimal amount of heat exchanged along a stochastic trajectory reads $dQ = \partial_x V\, dx$. Thus, we measure the heat exchanged between the particle and

the thermal bath during the interval $[t_i - \delta, t_i + \delta]$, which reads:

$$Q_i = V_{\rm ot}\left(x\left(t_i + \delta\right), t_i^-\right) - V_{\rm ot}\left(x\left(t_i - \delta\right), t_i^-\right) \ . \tag{6.9}$$

where $\delta = 20$ ms is significantly smaller than particle's relaxation time in the trap γ/k (60 ms), thus the heat values are before relaxation.

We then proceeded to test the non-equilibrium relations as given in Eqs. (6.6), Eq. (6.7), and Eq. (6.3) in an active bath employing the same protocol. We realize the active bath by using a bacterial bath, as in the experiments presented in the previous section.

In a first attempt, we use the optical potential $V_{\rm ot}$ and introduce an effective temperature to account for the additional fluctuations introduced by the active bath. Doing so, we obtain an effective temperature $T_{\rm eff} = 810\,\mathrm{K}$ and consequently an effective energy scale $\beta_{\rm eff} = (k_{\rm B}T_{\rm eff})^{-1}$, which we employ in Eq. (6.6). Importantly, the formulas to calculate the work applied on a particle (Eq. (6.8)) and heat exchange (Eq. (6.9)) are the same as in the case of the thermal bath described above. The resulting work distribution is represented by the symbols in Fig. 6.1c. This distribution is not Gaussian, differently from the work distribution in the case of a thermal bath. In order to validate Crooks fluctuation theorem (Eq. (6.6)), we estimate $P(+W)/P(-W)$, shown by the symbols in Fig. 6.1d. We observe a clear deviation (particularly towards the tails) from the expected value (solid line in Fig. 6.1d), which shows that Crooks fluctuation theorem is violated. We therefore conclude that the introduction of an effective temperature is not sufficient to employ non-equilibrium relations in an active bath. We remark that, even though the break-down of Crooks fluctuation theorem reported in Fig. (6.1d) can be theoretically predicted from the Boltzmann potential, one of the central results of the current work is to show experimentally that this break-down occurs for accessible parameter and can be quantified.

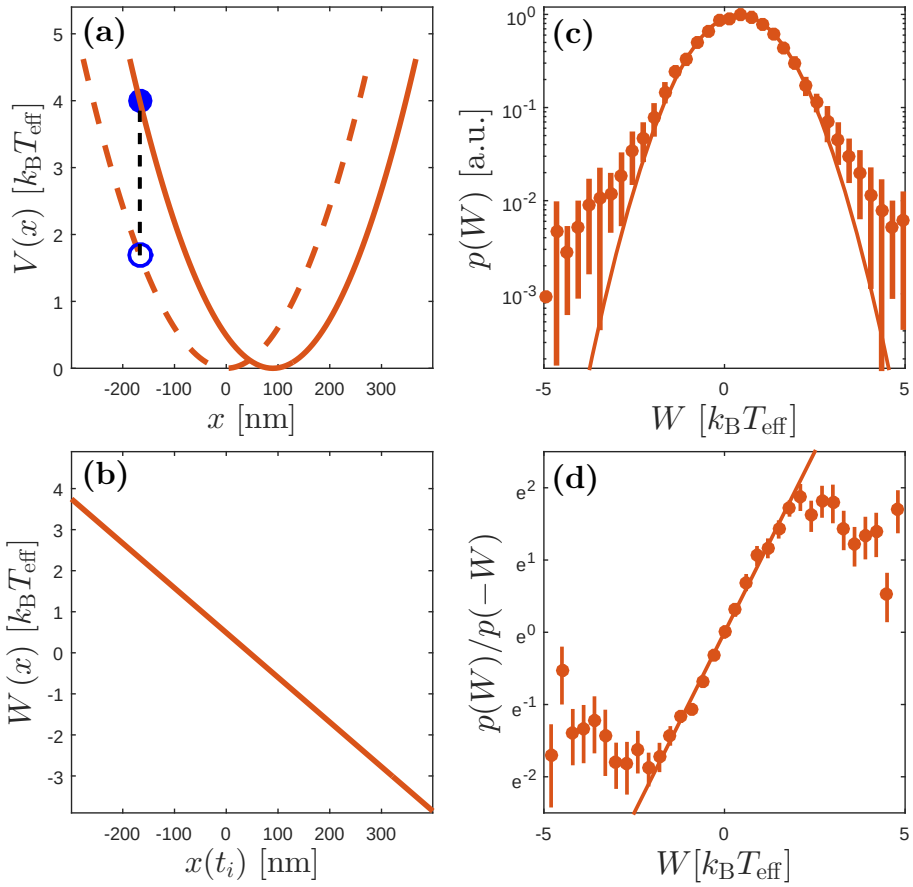

Figure 6.1: **Violation of Crooks fluctuation theorem in an active bath.** (a) The driving protocol entails an instantaneous translation of the trapping potential: the red dashed line represents the potential before switching, the red solid line the potential after switching, and the black dashed line the applied work. (b) Applied work as a function of the position of the particle before the potential translation. (c) Experimental probability distribution of work when the protocol shown in (a) is employed on a Brownian particle (silica, diameter $2R = 4.23 \pm 0.20\,\mu$m) held in an optical trap ($k = 1.33\,\mathrm{fN\,nm^{-1}}$) in an active (bacterial) bath, calculated using Eq. (6.8). The solid line represents the best Gaussian fit. (d) The red symbols show the ratio of the inverse work probabilities on the particle in active bath; they feature a clear deviation from Crooks fluctuation theorem (solid line, Eq. (6.6)). The data are obtained from 5000 work measurements; the error bars are obtained by repeating the measurements three times.

Therefore, in order to introduce a version of non-equilibrium relations working in active baths, we proceed to introduce an effective potential measured from the stationary particle distribution:

$$V_{\text{eff}}(x,\lambda) = -k_{\text{B}}T \log\left(\frac{p^{\text{s}}(x,\lambda)}{p^{\text{s}}(0,\lambda)}\right) \ , \tag{6.10}$$

where $p^{\text{s}}(x,\lambda)$ denotes the particle's stationary probability distribution under constant control parameter λ. An equivalent method was originally proposed by Hatano and Sasa for nonequilibrium steady states [50] and experimentally verified for the case of a system in a nonequilibrium steady state [60]. We experimentally measured V_{eff} (Fig. 6.2a) by fitting the stationary distribution to a q-Gaussian function ($q = 1.116$). In this approach, Eq. (6.8) for the work applied on the particle when the potential is switched must be changed to

$$W_i = V_{\text{eff}}\left(x\left(t_i\right), t_i^{+}\right) - V_{\text{eff}}\left(x\left(t_i\right), t_i^{-}\right) \ . \tag{6.11}$$

The amount of work we apply during a switch as a function of the position of the particle at switching time is shown in Fig. 6.2b and the resulting work distribution is shown in Fig. 6.2c; note the difference of the applied work using the effective potential (Fig. 6.2b) when compared with that using the optical potential (Fig. 6.1b), particularly in the tails of the distributions. Following from this work distribution we calculated $P(+W)/P(-W)$, which is shown by the symbols in Fig. 6.2d. The effective potential approach enables us to recover the Crooks fluctuation theorem in an active bath, as can be seen from the fact the measured values (symbols in Fig. 6.2d) are in good agreement with the theoretical prediction (line in Fig. 6.2d).

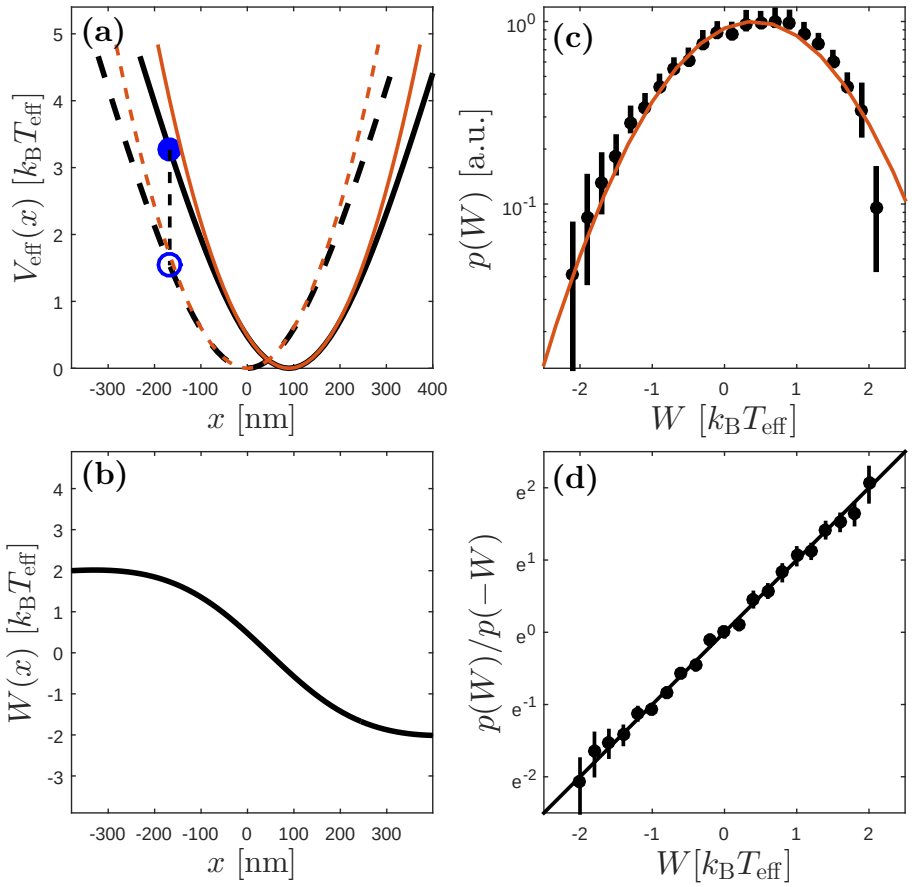

Figure 6.2: **Recovery of Crooks fluctuation theorem in an active bath using effective potentials.** (a) The driving protocol is the same as in Fig. 6.1a, but effective potentials obtained form the particle's stationary position distribution (black lines) are employed instead of the optical potentials (red lines). The difference between the effective and the optical potentials is particularly evident in the tails. (b) Applied work as a function of the position of the particle before the potential translation. (c) Experimental probability distribution of work when the protocol shown in (a) is employed on a Brownian particle (silica, diameter $2R = 4.23 \pm 0.20\,\mu$m) held in an optical trap ($k = 1.33\,\mathrm{fN\,nm^{-1}}$) in an active (bacterial) bath, calculated with the effective potential approach (Eq. (6.11)). The solid line is the same Gaussian fit as in Fig. 6.1c. (d) The black symbols show the ratio of the inverse work probabilities on the particle in active bath: the use of effective potentials recovers Crooks fluctuation theorem (solid line, Eq. (6.6)). The data are obtained from 5000 work measurements; the error bars are obtained by repeating the measurements three times.

To further corroborate the usefulness of the effective potential approach, we have also tested Jarzynski equality (Eq. (6.7) and the integral fluctuation theorem (Eq. (6.3). Figure 6.3a shows that Jarzynski equality is satisfied for large values of τ (we remind the reader that τ is the time interval between two successive switches of the potential), i.e., when the particle has enough time to reach a stationary state after switching the potential. Figure 6.3b shows that also the integral fluctuation theorem is validated when τ is large enough, as long as the formula for the heat (Eq. (6.9)) is calculated taking into account the effective potential, i.e.,

$$Q_i = V_{\text{eff}}\left(x\left(t_i+\delta\right), t_i^-\right) - V_{\text{eff}}\left(x\left(t_i-\delta\right), t_i^-\right). \tag{6.12}$$

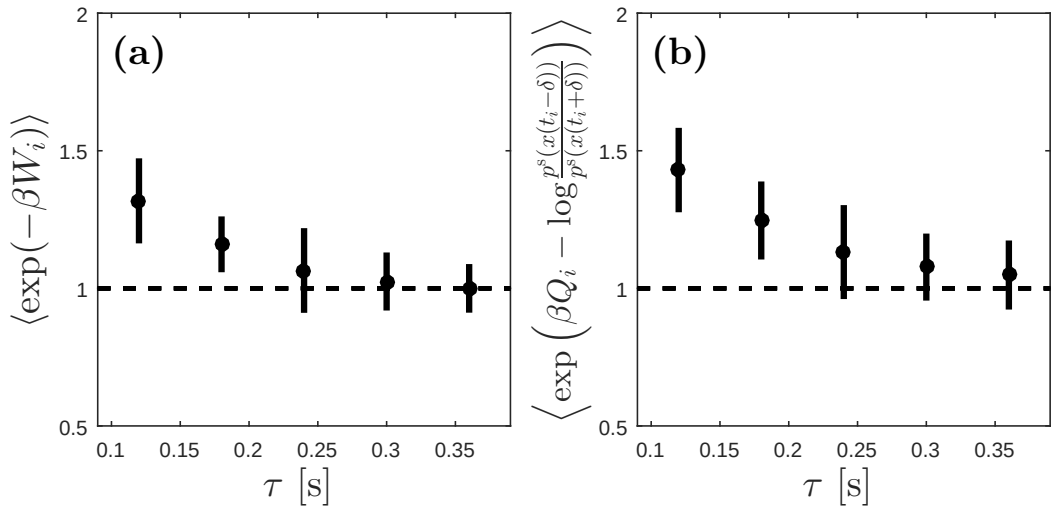

Figure 6.3: **Verification of Jarzynski equality and integral fluctuation theorem in an active bath using effective potential.** (a) Boltzmann weighted average of the applied work as a function of the waiting time τ between switches of the potential. If the particle is given enough time to reach a stationary state, Jarzynski equality (Eq. (6.7)) is satisfied. Dots represent the average over all measured work values for each τ. Rightmost dots ($\tau = 360\,\mathrm{ms}$) correspond to the work distribution in Fig. 6.2c. (b) Verification of the integral fluctuation theorem using effective potentials. Applied heat values are calculated from each switch using Eq. (6.3). The data are obtained from 5000 work measurements, the error bars are obtained by repeating the measurements three times.

It is important to underline that the recovery of the integral fluctuation theorem (Eq. (6.3) is a more general result than Crooks fluctuation theorem and Jarzynsky equality as it also verifies that the fluctuations before equilibration obey the theorem within the context of effective potentials.

Chapter 7

Conclusion

In the introductory chapters, I started with an overview of fundamental properties of stochastic thermodynamics with theoritical derivations and numerical examples where I also provided an overview of recent progress in this field. Following the introduction to stochastic thermodynamics, I discussed how fluctuation theorems are formulated when a thermal system is driven arbitrarily out of equilibrium. I supplied numerical examples as well as a comprehensive overview the literature. Finally, I explained the difference between thermal baths and active baths, where the system goes beyond the Markovian limit. I explained how the length scales of such systems are crucial when compared to the trapping length scales.

In the chapters where I presented our results, I showed that in an active bath, when a system is confined within a potential whose length scale is comparable or smaller than the characteristic length scale associated with the active noise, non-Boltzmann statistics emerge. The introduction of an effective temperature is not sufficient to provide a framework within which to describe such systems. Such framework can be instead provided by the use of an effective potential related to the system stationary distribution. This effective potential plays the same role as the mechanical potential; in particular, stochastic work and heat can be obtained from it, and such quantities turn out to satisfy the same fluctuation relations as the corresponding quantities in the passive bath case. We have exemplified

these results with a series of experiments using an optically trapped particle in an active (bacterial) bath.

Since active matter plays a central role in many systems, including very importantly living systems, our findings pose some significant limitations to the possibility of applying non-equilibrium fluctuation relations in their classical formulation to study this broad and valuable class of systems, pointing to the need for alternative approaches that explicitly model the presence of non-thermal fluctuations.

This work is expected to be followed by further studies within the same line of research. We have plans to explore the non-equilibrium relations of active baths when we also change the length scales of the trapping potential during a process, i.e, when we change our stiffness of the trap. Another important future work is to focus on information-to-heat conversion in the presense of active noise, where it may or may not obey the existing limits with regards to thermal baths.

Bibliography

[1] K. Huang, "Statistical mechanics," *New YorkLondon*, 1963.

[2] R. Landauer, "Irreversibility and heat generation in the computing process," *IBM journal of research and development*, vol. 5, no. 3, pp. 183–191, 1961.

[3] D. J. Evans, E. Cohen, and G. Morriss, "Probability of second law violations in shearing steady states," *Physical Review Letters*, vol. 71, no. 15, p. 2401, 1993.

[4] C. Jarzynski, "Nonequilibrium equality for free energy differences," *Physical Review Letters*, vol. 78, no. 14, p. 2690, 1997.

[5] G. E. Crooks, "Entropy production fluctuation theorem and the nonequilibrium work relation for free energy differences," *Physical Review E*, vol. 60, no. 3, p. 2721, 1999.

[6] U. Seifert, "Entropy production along a stochastic trajectory and an integral fluctuation theorem," *Physical review letters*, vol. 95, no. 4, p. 040602, 2005.

[7] J. Liphardt, S. Dumont, S. B. Smith, I. T. Jr., and C. Bustamante, "Equilibrium information from nonequilibrium measurements in an experimental test of Jarzynski's equality," *Science*, vol. 296, pp. 1832–1835, 2002.

[8] D. Collin, F. Ritort, C. Jarzynski, S. B. Smith, I. Tinoco, and C. Bustamante, "Verification of the Crooks fluctuation theorem and recovery of RNA folding free energies," *Nature*, vol. 437, pp. 231–234, 2005.

[9] R. Berkovich, J. Klafter, and M. Urbakh, "Analyzing friction forces with the jarzynski equality," *Journal of Physics: Condensed Matter*, vol. 20, no. 35, p. 354008, 2008.

[10] F. Douarche, S. Ciliberto, A. Petrosyan, and I. Rabbiosi, "An experimental test of the jarzynski equality in a mechanical experiment," *EPL (Europhysics Letters)*, vol. 70, no. 5, p. 593, 2005.

[11] V. Blickle, T. Speck, L. Helden, U. Seifert, and C. Bechinger, "Thermodynamics of a colloidal particle in a time-dependent nonharmonic potential," *Physical review letters*, vol. 96, no. 7, p. 070603, 2006.

[12] M. Cates, "Diffusive transport without detailed balance in motile bacteria: does microbiology need statistical physics?," *Reports on Progress in Physics*, vol. 75, no. 4, p. 042601, 2012.

[13] C. Bechinger, R. Di Leonardo, H. Löwen, C. Reichhardt, G. Volpe, and G. Volpe, "Active brownian particles in complex and crowded environments," *arXiv preprint arXiv:1602.00081*, 2016.

[14] J. R. Howse, R. A. Jones, A. J. Ryan, T. Gough, R. Vafabakhsh, and R. Golestanian, "Self-motile colloidal particles: from directed propulsion to random walk," *Physical review letters*, vol. 99, no. 4, p. 048102, 2007.

[15] E. Ben-Isaac, Y. Park, G. Popescu, F. L. H. Brown, N. S. Gov, and Y. Shokef, "Effective temperature of red-blood-cell membrane fluctuations," *Phys. Rev. Lett.*, vol. 106, p. 238103, 2011.

[16] D. Loi, S. Mossa, and L. F. Cugliandolo, "Effective temperature of active matter," *Phys. Rev. E*, vol. 77, p. 051111, 2008.

[17] E. Pinçe, S. K. Velu, A. Callegari, P. Elahi, S. Gigan, G. Volpe, and G. Volpe, "Disorder-mediated crowd control in an active matter system," *Nature communications*, vol. 7, 2016.

[18] N. Koumakis, A. Lepore, C. Maggi, and R. Di Leonardo, "Targeted delivery of colloids by swimming bacteria," *Nature communications*, vol. 4, 2013.

[19] S. Carnot, "Reflections on the motive power of fire, and on machines fitted to develop that power," *Paris: Bachelier*, 1824.

[20] R. Clausius, "Über verschiedene für die anwendung bequeme formen der hauptgleichungen der mechanischen wärmetheorie," *Annalen der Physik*, vol. 201, no. 7, pp. 353–400, 1865.

[21] J. W. Gibbs, "On the equilibrium of heterogeneous substances," *American Journal of Science*, no. 96, pp. 441–458, 1878.

[22] P. Langevin, "Cr acad. sci.(paris) 146, 530; trans. lemons, ds & gythiel, a.(1997)," *Am. J. Phys*, vol. 65, pp. 1079–1081, 1908.

[23] A. Einstein, "Un the movement of small particles suspended in statiunary liquids required by the molecular-kinetic theory 0f heat," *Ann. Phys*, vol. 17, pp. 549–560, 1905.

[24] E. M. Purcell, "Life at low reynolds number," *Am. J. Phys*, vol. 45, no. 1, pp. 3–11, 1977.

[25] B. Øksendal, "Stochastic differential equations," in *Stochastic differential equations*, pp. 65–84, Springer, 2003.

[26] E. Platen, "An introduction to numerical methods for stochastic differential equations," *Acta numerica*, vol. 8, pp. 197–246, 1999.

[27] G. Volpe and G. Volpe, "Simulation of a brownian particle in an optical trap," *American Journal of Physics*, vol. 81, no. 3, pp. 224–230, 2013.

[28] A. Shiryayev, "On analytical methods in probability theory," in *Selected works of AN Kolmogorov*, pp. 62–108, Springer, 1992.

[29] K. Sekimoto, "Langevin equation and thermodynamics," *Progress of Theoretical Physics Supplement*, vol. 130, pp. 17–27, 1998.

[30] K. Sekimoto, *Stochastic energetics*, vol. 799. Springer, 2010.

[31] I. A. Martínez, É. Roldán, L. Dinis, D. Petrov, and R. A. Rica, "Adiabatic processes realized with a trapped brownian particle," *Physical review letters*, vol. 114, no. 12, p. 120601, 2015.

[32] P. Hänggi and F. Marchesoni, "Artificial brownian motors: Controlling transport on the nanoscale," *Reviews of Modern Physics*, vol. 81, no. 1, p. 387, 2009.

[33] C. S. Peskin, G. M. Odell, and G. F. Oster, "Cellular motions and thermal fluctuations: the brownian ratchet.," *Biophysical journal*, vol. 65, no. 1, p. 316, 1993.

[34] U. Seifert, "Stochastic thermodynamics, fluctuation theorems and molecular machines," *Reports on Progress in Physics*, vol. 75, no. 12, p. 126001, 2012.

[35] C. Jarzynski, "Equalities and inequalities: irreversibility and the second law of thermodynamics at the nanoscale," *Annu. Rev. Condens. Matter Phys.*, vol. 2, no. 1, pp. 329–351, 2011.

[36] V. Blickle and C. Bechinger, "Realization of a micrometre-sized stochastic heat engine," *Nature Physics*, vol. 8, no. 2, pp. 143–146, 2012.

[37] I. A. Martínez, É. Roldán, L. Dinis, D. Petrov, J. M. Parrondo, and R. A. Rica, "Brownian carnot engine," *Nature Physics*, vol. 12, no. 1, pp. 67–70, 2016.

[38] P. A. Quinto-Su, "A microscopic steam engine implemented in an optical tweezer," *Nature communications*, vol. 5, 2014.

[39] S. Krishnamurthy, S. Ghosh, D. Chatterji, R. Ganapathy, and A. Sood, "A micrometer-sized heat engine operating between bacterial reservoirs," *arXiv preprint arXiv:1601.03130*, 2016.

[40] T. Schmiedl and U. Seifert, "Efficiency at maximum power: An analytically solvable model for stochastic heat engines," *EPL (Europhysics Letters)*, vol. 81, no. 2, p. 20003, 2007.

[41] S. Robert, "Patent no. 4081," *Stirling air engine and the heat regenerator*, 1816.

[42] P. Jones, O. Maragó, and G. Volpe, *Optical tweezers: Principles and applications*. Cambridge University Press, 2015.

[43] M. L. Cordero, E. Verneuil, F. Gallaire, and C. N. Baroud, "Time-resolved temperature rise in a thin liquid film due to laser absorption," *Physical Review E*, vol. 79, no. 1, p. 011201, 2009.

[44] G. Gallavotti and E. Cohen, "Dynamical ensembles in nonequilibrium statistical mechanics," *Physical Review Letters*, vol. 74, no. 14, p. 2694, 1995.

[45] D. J. Evans and D. J. Searles, "Equilibrium microstates which generate second law violating steady states," *Physical Review E*, vol. 50, no. 2, p. 1645, 1994.

[46] J. L. Lebowitz and H. Spohn, "A gallavotti–cohen-type symmetry in the large deviation functional for stochastic dynamics," *Journal of Statistical Physics*, vol. 95, no. 1-2, pp. 333–365, 1999.

[47] J. Kurchan, "Fluctuation theorem for stochastic dynamics," *Journal of Physics A: Mathematical and General*, vol. 31, no. 16, p. 3719, 1998.

[48] C. Jarzynski, "Equilibrium free-energy differences from nonequilibrium measurements: A master-equation approach," *Physical Review E*, vol. 56, no. 5, p. 5018, 1997.

[49] G. E. Crooks, "Nonequilibrium measurements of free energy differences for microscopically reversible markovian systems," *Journal of Statistical Physics*, vol. 90, no. 5-6, pp. 1481–1487, 1998.

[50] T. Hatano and S.-i. Sasa, "Steady-state thermodynamics of langevin systems," *Physical review letters*, vol. 86, no. 16, p. 3463, 2001.

[51] G. Hummer and A. Szabo, "Free energy reconstruction from nonequilibrium single-molecule pulling experiments," *Proceedings of the National Academy of Sciences*, vol. 98, no. 7, pp. 3658–3661, 2001.

[52] G. E. Crooks, "Path-ensemble averages in systems driven far from equilibrium," *Physical review E*, vol. 61, no. 3, p. 2361, 2000.

[53] A. B. Adib, "Entropy and density of states from isoenergetic nonequilibrium processes," *Physical Review E*, vol. 71, no. 5, p. 056128, 2005.

[54] D. J. Evans and D. J. Searles, "The fluctuation theorem," *Advances in Physics*, vol. 51, no. 7, pp. 1529–1585, 2002.

[55] G. Hummer and A. Szabo, "Free energy surfaces from single-molecule force spectroscopy," *Accounts of chemical research*, vol. 38, no. 7, pp. 504–513, 2005.

[56] F. Ritort, "Single-molecule experiments in biological physics: methods and applications," *Journal of Physics: Condensed Matter*, vol. 18, no. 32, p. R531, 2006.

[57] T. Speck and U. Seifert, "Integral fluctuation theorem for the housekeeping heat," *Journal of Physics A: Mathematical and General*, vol. 38, no. 34, p. L581, 2005.

[58] A. N. Gupta, A. Vincent, K. Neupane, H. Yu, F. Wang, and M. T. Woodside, "Experimental validation of free-energy-landscape reconstruction from non-equilibrium single-molecule force spectroscopy measurements," *Nature Physics*, vol. 7, no. 8, pp. 631–634, 2011.

[59] N. C. Harris, Y. Song, and C.-H. Kiang, "Experimental free energy surface reconstruction from single-molecule force spectroscopy using jarzynskis equality," *Physical review letters*, vol. 99, no. 6, p. 068101, 2007.

[60] E. Trepagnier, C. Jarzynski, F. Ritort, G. E. Crooks, C. Bustamante, and J. Liphardt, "Experimental test of hatano and sasa's nonequilibrium steady-state equality," *Proceedings of the National Academy of Sciences of the United States of America*, vol. 101, no. 42, pp. 15038–15041, 2004.

[61] S. Schuler, T. Speck, C. Tietz, J. Wrachtrup, and U. Seifert, "Experimental test of the fluctuation theorem for a driven two-level system with time-dependent rates," *Physical review letters*, vol. 94, no. 18, p. 180602, 2005.

[62] S. An, J.-N. Zhang, M. Um, D. Lv, Y. Lu, J. Zhang, Z.-Q. Yin, H. Quan, and K. Kim, "Experimental test of the quantum jarzynski equality with a trapped-ion system," *Nature Physics*, vol. 11, no. 2, pp. 193–199, 2015.

[63] X.-D. Shang, P. Tong, and K.-Q. Xia, "Test of steady-state fluctuation theorem in turbulent rayleigh-bénard convection," *Physical Review E*, vol. 72, no. 1, p. 015301, 2005.

[64] O.-P. Saira, Y. Yoon, T. Tanttu, M. Möttönen, D. Averin, and J. P. Pekola, "Test of the jarzynski and crooks fluctuation relations in an electronic system," *Physical review letters*, vol. 109, no. 18, p. 180601, 2012.

[65] A. Ashkin, J. Dziedzic, J. Bjorkholm, and S. Chu, "Observation of a single-beam gradient force optical trap for dielectric particles," *Optics letters*, vol. 11, no. 5, pp. 288–290, 1986.

[66] G. Volpe, G. Volpe, and D. Petrov, "Brownian motion in a nonhomogeneous force field and photonic force microscope," *Physical Review E*, vol. 76, no. 6, p. 061118, 2007.

[67] S. Ramaswamy, "The mechanics and statistics of active matter," *Annual Review of Condensed Matter Physics*, vol. 1, pp. 323–345, 2010.

[68] U. Erdmann, W. Ebeling, L. Schimansky-Geier, and F. Schweitzer, "Brownian particles far from equilibrium," *The European Physical Journal B-Condensed Matter and Complex Systems*, vol. 15, no. 1, pp. 105–113, 2000.

[69] M. Hauser and L. Schimansky-Geier, "Statistical physics of self-propelled particles," *The European Physical Journal Special Topics*, vol. 224, no. 7, pp. 1147–1150, 2015.

[70] F. Schweitzer and J. D. Farmer, *Brownian agents and active particles: collective dynamics in the natural and social sciences*. Springer Science & Business Media, 2007.

[71] P. Romanczuk, M. Bär, W. Ebeling, B. Lindner, and L. Schimansky-Geier, "Active brownian particles," *The European Physical Journal Special Topics*, vol. 202, no. 1, pp. 1–162, 2012.

[72] H. C. Berg, *E. coli in Motion*. Springer Science & Business Media, 2008.

[73] J. Tailleur and M. Cates, "Statistical mechanics of interacting run-and-tumble bacteria," *Physical review letters*, vol. 100, no. 21, p. 218103, 2008.

[74] M. Cates and J. Tailleur, "When are active brownian particles and run-and-tumble particles equivalent? consequences for motility-induced phase separation," *EPL (Europhysics Letters)*, vol. 101, no. 2, p. 20010, 2013.

[75] S. J. Ebbens and J. R. Howse, "In pursuit of propulsion at the nanoscale," *Soft Matter*, vol. 6, no. 4, pp. 726–738, 2010.

[76] R. F. Ismagilov, A. Schwartz, N. Bowden, and G. M. Whitesides, "Autonomous movement and self-assembly," *Angewandte Chemie International Edition*, vol. 41, no. 4, pp. 652–654, 2002.

[77] W. F. Paxton, K. C. Kistler, C. C. Olmeda, A. Sen, S. K. St. Angelo, Y. Cao, T. E. Mallouk, P. E. Lammert, and V. H. Crespi, "Catalytic nanomotors: autonomous movement of striped nanorods," *Journal of the American Chemical Society*, vol. 126, no. 41, pp. 13424–13431, 2004.

[78] H.-R. Jiang, N. Yoshinaga, and M. Sano, "Active motion of a janus particle by self-thermophoresis in a defocused laser beam," *Physical review letters*, vol. 105, no. 26, p. 268302, 2010.

[79] I. Buttinoni, G. Volpe, F. Kümmel, G. Volpe, and C. Bechinger, "Active brownian motion tunable by light," *Journal of Physics: Condensed Matter*, vol. 24, no. 28, p. 284129, 2012.

[80] G. E. Uhlenbeck and L. S. Ornstein, "On the theory of the brownian motion," *Physical review*, vol. 36, no. 5, p. 823, 1930.

[81] T. Li, S. Kheifets, D. Medellin, and M. G. Raizen, "Measurement of the instantaneous velocity of a brownian particle," *Science*, vol. 328, no. 5986, pp. 1673–1675, 2010.

[82] S. Kheifets, A. Simha, K. Melin, T. Li, and M. G. Raizen, "Observation of brownian motion in liquids at short times: instantaneous velocity and memory loss," *science*, vol. 343, no. 6178, pp. 1493–1496, 2014.

[83] R. Huang, I. Chavez, K. M. Taute, B. Lukić, S. Jeney, M. G. Raizen, and E.-L. Florin, "Direct observation of the full transition from ballistic to diffusive

brownian motion in a liquid," *Nature Physics*, vol. 7, no. 7, pp. 576–580, 2011.

[84] G. Grégoire, H. Chaté, and Y. Tu, "Active and passive particles: Modeling beads in a bacterial bath," *Physical Review E*, vol. 64, no. 1, p. 011902, 2001.

[85] X.-L. Wu and A. Libchaber, "Particle diffusion in a quasi-two-dimensional bacterial bath," *Physical Review Letters*, vol. 84, no. 13, p. 3017, 2000.

[86] N. Koumakis, C. Maggi, and R. Di Leonardo, "Directed transport of active particles over asymmetric energy barriers," *Soft matter*, vol. 10, no. 31, pp. 5695–5701, 2014.

[87] G. Volpe, I. Buttinoni, D. Vogt, H.-J. Kümmerer, and C. Bechinger, "Microswimmers in patterned environments," *Soft Matter*, vol. 7, no. 19, pp. 8810–8815, 2011.

[88] A. Kaiser, H. Wensink, and H. Löwen, "How to capture active particles," *Physical review letters*, vol. 108, no. 26, p. 268307, 2012.

[89] P. Galajda, J. Keymer, P. Chaikin, and R. Austin, "A wall of funnels concentrates swimming bacteria," *Journal of bacteriology*, vol. 189, no. 23, pp. 8704–8707, 2007.

[90] M. E. Cates and J. Tailleur, "Motility-induced phase separation," *arXiv preprint arXiv:1406.3533*, 2014.

[91] A. Suma, G. Gonnella, D. Marenduzzo, and E. Orlandini, "Motility-induced phase separation in an active dumbbell fluid," *EPL (Europhysics Letters)*, vol. 108, no. 5, p. 56004, 2014.

[92] C. Reichhardt and C. J. O. Reichhardt, "Absorbing phase transitions and dynamic freezing in running active matter systems," *Soft matter*, vol. 10, no. 38, pp. 7502–7510, 2014.

[93] R. Di Leonardo, L. Angelani, D. DellArciprete, G. Ruocco, V. Iebba, S. Schippa, M. Conte, F. Mecarini, F. De Angelis, and E. Di Fabrizio,

"Bacterial ratchet motors," *Proceedings of the National Academy of Sciences*, vol. 107, no. 21, pp. 9541–9545, 2010.

[94] C. Maggi, J. Simmchen, F. Saglimbeni, J. Katuri, M. Dipalo, F. De Angelis, S. Sanchez, and R. Di Leonardo, "Self-assembly of micromachining systems powered by janus micromotors," *Small*, vol. 12, no. 4, pp. 446–451, 2016.

[95] J. W. Gibbs, *Elementary principles of statistical mechanics*. New Haven: Yale University Press, 1902.

[96] G. M. Wang, E. M. Sevick, E. Mittag, D. J. Searles, and D. J. Evans, "Experimental demonstration of violations of the second law of thermodynamics for small systems and short time scales," *Phys. Rev. Lett.*, vol. 89, p. 050601, 2002.

[97] E. Barkai, Y. Garini, and R. Metzler, "Strange kinetics of single molecules in living cells," *Phys. Today*, vol. 65, pp. 29–35, 2012.

[98] S. Ciliberto, A. Imparato, A. Naert, and M. Tanase, "Heat flux and entropy produced by thermal fluctuations," *Phys. Rev. Lett.*, vol. 110, p. 180601, 2013.

[99] A. Bérut, A. Imparato, A. Petrosyan, and S. Ciliberto, "Stationary and transient fluctuation theorems for effective heat fluxes between hydrodynamically coupled particles in optical traps," *Phys. Rev. Lett.*, vol. 116, p. 068301, 2016.

[100] J. Harder, C. Valeriani, and A. Cacciuto, "Activity-induced collapse and reexpansion of rigid polymers," *Phys. Rev. E*, vol. 90, p. 062312, 2014.

[101] R. Suzuki, C. A. Weber, E. Frey, and A. R. Bausch, "Polar pattern formation in driven filament systems requires non-binary particle collisions," *Nat. Phys.*, vol. 11, pp. 839–843, 2015.

[102] S. A. Mallory, C. Valeriani, and A. Cacciuto, "Anomalous dynamics of an elastic membrane in an active fluid," *Phys. Rev. E*, vol. 92, p. 012314, 2015.

[103] J. Shin, A. G. Cherstvy, W. K. Kim, and R. Metzler, "Facilitation of polymer looping and giant polymer diffusivity in crowded solutions of active particles," *New J. Phys.*, vol. 17, p. 113008, 2015.

[104] R. Parthasarathy, "Rapid, accurate particle tracking by calculation of radial symmetry centers," *Nat. Methods*, vol. 9, pp. 724–726, 2012.

[105] N. Koumakis, C. Maggi, and R. Di Leonardo, "Directed transport of active particles over asymmetric energy barriers," *Soft Matter*, vol. 10, pp. 5695–5701, 2014.

[106] Z. Wang, H. Y. Chen, Y. J. Sheng, and H. K. Tsao, "Diffusion, sedimentation equilibrium, and harmonic trapping of run-and-tumble nanoswimmers," *Soft Matter*, vol. 10, no. 18, pp. 3209–3217, 2014.

[107] D. T. Chen, A. Lau, L. A. Hough, M. F. Islam, M. Goulian, T. C. Lubensky, and A. G. Yodh, "Fluctuations and rheology in active bacterial suspensions," *Physical Review Letters*, vol. 99, no. 14, p. 148302, 2007.

[108] C. Maggi, M. Paoluzzi, N. Pellicciotta, A. Lepore, L. Angelani, and R. Di Leonardo, "Generalized energy equipartition in harmonic oscillators driven by active baths," *Phys. Rev. Lett.*, vol. 113, p. 238303, 2014.

[109] C. Tsallis, *Introduction to nonextensive statistical mechanics*. Heidelberg, Germany: Springer Verlag, 2009.

[110] G. B. Bagci and T. Oikonomou, "Tsallis power laws and finite baths with negative heat capacity," *Phys. Rev. E*, vol. 88, no. 4, p. 042126, 2013.

[111] A. Bricard, J. B. Caussin, D. Das, C. Savoie, V. Chikkadi, K. Shitara, O. Chepizhko, F. Peruani, D. Saintillan, and D. Bartolo, "Emergent vortices in populations of colloidal rollers," *Nat. Commun.*, vol. 6, p. 7470, 2015.

[112] J. Tailleur and M. E. Cates, "Sedimentation, trapping, and rectification of dilute bacteria," *EPL (Europhysics Letters)*, vol. 86, no. 6, p. 60002, 2009.

[113] L. Angelani and R. Di Leonardo, "Geometrically biased random walks in bacteria-driven micro-shuttles," *New J. Phys.*, vol. 12, p. 113017, 2010.

[114] K. Sekimoto, *Stochastic Energetics*. Lecture Notes in Physics, Heidelberg, Germany: Springer Verlag, 2010.

Appendix A

Experimental Methods

Here, the experimental methods that are employed within the experiments described in this thesis will be covered under 3 sections, I will begin with introducing the experimental setup. Then I will focus on bacterial bath preparation and how we prepared experimental samples. Finally, I will explain the methods that are used to acquire and analyze the data we acquired.

A.1 Optical trapping and experimental setup

Optical tweezers is a technique where light's momentum can be used to manipulate microscopic objects in water [42]. We employed this technique in order to conduct our experiments. This technique requires focusing a Gaussian beam with a high a high-numerical aperture objective. This creates a trapping harmonic potential for a Brownian particle immersed in watery solutions. In order to be able to modulate our trapping potential, we employed a spatial light modulator. The zero order of the laser beam on the light modulator is eliminated by 4F method. The experimental setup is represented schematically in Fig. A.1.

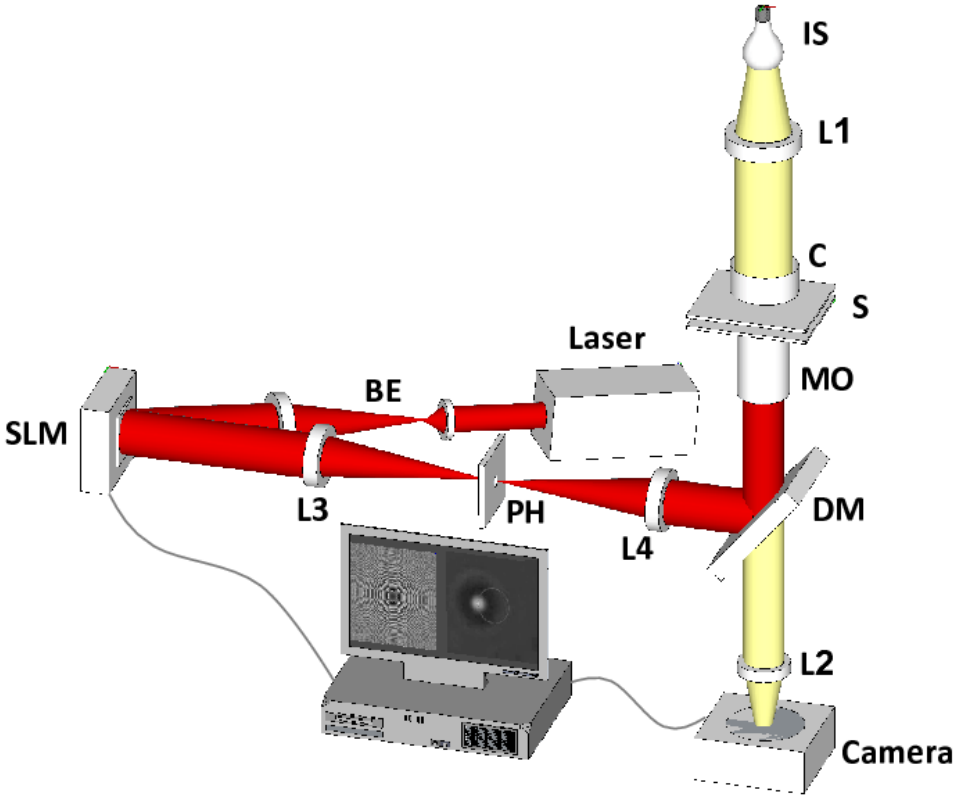

Figure A.1: **Schematic of the experimental setup.** The optical setup is based on a holographic optical tweezers and a digital video microscope. IS: Illumination source. L1: Collecting lens. C: Condenser. S: Sample chamber. MO: Microscope objective. DM: Dichroic mirror. L2: Tube lens. BE: Beam expander. SLM: Spatial light modulator. L3 and L4: lenses for 4f-configuration. PH: Pinhole.

A.2 Bacterial sample preparation

We store wild-type strain RP437 *Escherichia coli* bacteria as a solid culture delivered by Yale University *E. coli* Stock Center, which is kept at $-80°$C in the archive stock. In order to grow a culture, we inoculate the bacteria on an agar plate which is a sterilized medium. Then, we incubate the agar place overnight at 32.5°C temperature in order to grow single colonies. Single colonies were isolated and toothpicked from the plate and transferred into a fresh liquid (broth)

medium, which contains 1% tryptone. Then, a fresh tryptone broth was injected by 1:100 diluted sample taken at the stationary phase. After that, we let fresh tryptone solution reach to its middle growth phase (OD 600 $\sim$ 0.40) inside an incubator at 180 rpm and 32.5°C. We take the final solution is put into a falcon tube and centrifuge at 2000 rpm at lab temperature. Finally, we gently pick up the pellet RP437 cells by a sterilized pipet and re-suspend in a motility buffer. Motility buffer was prepared with 0.1 mM EDTA, 10 mM dextrose, 10 mM monobasic potassium phosphate (KH_2PO_4), and 0.002% of Tween 20.

A.3 Data analysis

Data we obtained during the experiments are acquired with Thorlabs CMOS cameras and analyzed by digital video microscopy. There are two typical tracking methods used for the analysis. First one is centroid tracking which requires tresholding of the image of the trapped particle and then taking the center of mass [42]. This method was used to analyze data that are presented in chapter 6. The second method we employed for tracking trapped particle is radial symmetry algorithm, which requires finding the gradient lines of the image intensity at multiple parts and determining the point which has smallest total distance to these lines [104]. The data that are presented in chapter 5 were obtained by this method.

Appendix B

Codes

B.1 Figure 2.1 - Demonstration of Boltzmann distribution for a confined Brownian particle

```
clear all; close all; clc;
% Simulation parameters:
T=300;                              % Temperature
kB=1.38e-23;                        % Boltzmann constant
nu=0.001;                           % Viscosity of water
R=1e-6;                             % Radius of the particle
gamma=6*pi*nu*R;                    % Friction coefficient
l=(-255:255)*1e-9;                  % Spacing
U1=kB*T*(l/(50e-9)).^2;             % Harmonic potential
U2=kB*T*(l/(92e-9)).^4;             % Quartic potential
U3=kB*T*((l/(77e-9)).^4 ...         % Double potential
-(l/(45e-9)).^2);
U3=U3-min(U3);                      % Making minimum value of the potential
dt=.5e-3;                           % Time Interval
```

```
N=10000000;                          % Number of iterations
x1=zeros(1,N);                       % Initial position
x2=zeros(1,N);
x3=zeros(1,N);
F1=-diff(U1)/(l(2)-l(1));            % Forces
F2=-diff(U2)/(l(2)-l(1));
F3=-diff(U3)/(l(2)-l(1));


for i=1:N

    j=find(x1(i)>l); i1=j(end);  % Finding force value
    j=find(x2(i)>l); i2=j(end);
    j=find(x3(i)>l); i3=j(end);

    x1(i+1)=x1(i) + F1(i1)/gamma*dt...  % Force due to potential
        +sqrt(2*kB*T*dt/gamma)*randn;   % Thermal noise term
    x2(i+1)=x2(i) + F2(i2)/gamma*dt...
        +sqrt(2*kB*T*dt/gamma)*randn;
    x3(i+1)=x3(i) + F3(i3)/gamma*dt...
        +sqrt(2*kB*T*dt/gamma)*randn;
end
ll=(-170:5:170)*1e-9;
P=hist(x1,ll); NP1=P/max(P);
P=hist(x2,ll); NP2=P/max(P);
P=hist(x3,ll); NP3=P/max(P);
TP1=exp(-U1/kB/T)/max(exp(-U1/kB/T));
TP2=exp(-U2/kB/T)/max(exp(-U2/kB/T));
TP3=exp(-U3/kB/T)/max(exp(-U3/kB/T));
```

B.2 Example 2.1 - Isochoric heating

```
clear all; close all; clc;
```

```
% Simulation parameters
T0=50;                          % Initial Temperature
TF=500;                         % Final Temperature
kB=1.38e-23;                    % Boltzmann constant
nu=0.001;                       % Viscosity of water
R=1e-6;                         % Radius of the particle
gamma=6*pi*nu*R;                % Friction coefficient
l=(-255:255)*1e-9;              % Spacing
k=1e-6;                         % Stifness
t=5;                            % Time of the process
dt=.5e-3;                       % Finite time difference
tR=2;                           % Relaxation time
N=t/dt;                         % Number of steps
n=1000000;
x=zeros(1,n);                   % Initial values
y=zeros(1,N);                   % Sample trajectories
Q=zeros(1,N);                   % heat exchange
Qy=zeros(size(y,1),N);
stdx=zeros(1,N);


for i=1:round(tR/dt)
    x=x-k/gamma*x*dt+sqrt(2*kB*T0*dt/gamma)*randn(1,n);
    y(:,1)=y(:,1)-k/gamma*y(:,1)*dt...
        +sqrt(2*kB*T0*dt/gamma)*randn(size(y,1),1);
end
xi=x;
stdx(1)=std(x);
for i=1:(N-1)
    dx=-k/gamma*x*dt...
        +sqrt(2*kB*(T0+i*(TF-T0)/N)*dt/gamma)*randn(1,n);
    Q(i+1)=Q(i)+mean(.5*k*((x+dx).^2-x.^2)/kB/T0);
    x=x+dx;
```

```
    stdx(i+1)=std(x);
    y(:,i+1)=y(:,i)-k/gamma*y(:,i)*dt...
    +sqrt(2*kB*(T0+i*(TF-T0)/N)*dt/gamma)*randn(size(y,1),1);
    Qy(:,i+1)=Qy(:,i)+.5*k*(y(:,i+1).^2-y(:,i).^2)/kB/T0;
end
```

B.3 Example 2.2 - Isothermal compression

```
clear all; close all; clc;
%% Simulating
T=300;                          % Constant Temperature
kB=1.38e-23;                    % Boltzmann constant
nu=0.001;                       % Viscosity of water
R=1e-6;                         % Radius of the particle
gamma=6*pi*nu*R;                % Friction coefficient
l=(-255:255)*1e-9;              % Spacing
k0=.1e-6;                       % Initial Stifness
kf=1e-6;                        %Final Stifness
t=.5;                           % Time of the process
dt=.5e-3;                       % Finite time difference
tR=5;                           % Relaxation time
N=t/dt;                         % Number of steps
n=1000000;
x=zeros(1,n);                   % Initial values
y=zeros(10,N);                  % Sample trajectories
W=zeros(1,N);                   % work applied in each iteration
Wy=zeros(size(y,1),N);
stdx=zeros(1,N);
dk=(kf-k0)/N;

for i=1:round(tR/dt)
    x=x-k0/gamma*x*dt+sqrt(2*kB*T*dt/gamma)*randn(1,n);
    y(:,1)=y(:,1)-k0/gamma*y(:,1)*dt...
```

```
        +sqrt(2*kB*T*dt/gamma)*randn(size(y,1),1);
end
xi=x;
stdx(1)=std(x);
for i=1:(N-1)
    dx=-(k0+(kf-k0)*i/N)/gamma*x*dt...
        +sqrt(2*kB*T*dt/gamma)*randn(1,n);
    W(i+1)=W(i)+mean(.5*dk*(x.^2)/kB/T);
    x=x+dx;
    stdx(i+1)=std(x);
    y(:,i+1)=y(:,i)-(k0+(kf-k0)*i/N)/gamma*y(:,i)*dt...
        +sqrt(2*kB*T*dt/gamma)*randn(size(y,1),1);
    Wy(:,i+1)=Wy(:,i)+.5*dk*y(:,i).^2/kB/T;
end
```

B.4 Example 3.1 - Crooks fluctuation theorem in an arbitrary process

```
clear all; close all; clc;

% Simulating
T=300;                          % Temperature
kB=1.38e-23;                    % Boltzmann constant
nu=0.001;                       % Viscosity of water
R=1e-6;                         % Radius of the particle
gamma=6*pi*nu*R;                % Friction coefficient
l=(-255:255)*1e-9;              % Spacing

kk=4*kB*T/(77e-9)^4;
k=2*kB*T/(45e-9).^2;
t=.2;
tR=2;
```

```
dt=.5e-3;
N1=round(t/dt);
lambda1=1:-(1/N1):0;
t=.05;
N2=round(t/dt);
lambda2=1:-(1/N2):0;
t=0.02;
N3=round(t/dt);
lambda3=1:-(1/N3):0;
n=10000;
x=zeros(1,n);
WF1=zeros(1,n); WF2=zeros(1,n); WF3=zeros(1,n);
WB1=zeros(1,n); WB2=zeros(1,n); WB3=zeros(1,n);
%forward protocol
for i=1:round(tR/dt)
    x=x-(kk*lambda1(1)*x.^3 ...
        +k*(1-2*lambda1(1))*x)*dt/gamma...
        +sqrt(2*kB*T*dt/gamma)*randn(1,n);
%       plot(x,'b.','MarkerSize',30); drawnow();
   disp(i);
end
y=x;

for i=1:N1
    x=x-(kk*lambda1(i)*x.^3 ...
        +k*(1-2*lambda1(i))*x)*dt/gamma ...
        +sqrt(2*kB*T*dt/gamma)*randn(1,n);
    WF1=WF1+kk*(lambda1(i+1)-lambda1(i))*x.^4/4/kB/T...
        -k*x.^2/kB/T*(lambda1(i+1)-lambda1(i));
end
x=y;
for i=1:N2
    x=x-(kk*lambda2(i)*x.^3 ...
```

```
        +k*(1-2*lambda2(i))*x)*dt/gamma  ...
        +sqrt(2*kB*T*dt/gamma)*randn(1,n);
    WF2=WF2+kk*(lambda2(i+1)-lambda2(i))*x.^4/4/kB/T...
        -k*x.^2/kB/T*(lambda2(i+1)-lambda2(i));
end
x=y;
for i=1:N3
    x=x-(kk*lambda3(i)*x.^3  ...
        +k*(1-2*lambda3(i))*x)*dt/gamma...
        +sqrt(2*kB*T*dt/gamma)*randn(1,n);
    WF3=WF3+kk*(lambda3(i+1)-lambda3(i))*x.^4/4/kB/T...
        -k*x.^2/kB/T*(lambda3(i+1)-lambda3(i));
end

%backward protocol
lambda1=0:(1/N1):1;
lambda2=0:(1/N2):1;
lambda3=0:(1/N3):1;
x=zeros(1,n);
for i=1:round(tR/dt)
    x=x-(kk*lambda1(1)*x.^3+k*(1-2*lambda1(1))*x)*dt/gamma...
        +sqrt(2*kB*T*dt/gamma)*randn(1,n);
%      plot(x,'b.','MarkerSize',30); drawnow();
end
y=x;

for i=1:N1
    x=x-(kk*lambda1(i)*x.^3+k*(1-2*lambda1(i))*x)*dt/gamma...
        +sqrt(2*kB*T*dt/gamma)*randn(1,n);
    WB1=WB1+kk*(lambda1(i+1)-lambda1(i))*x.^4/4/kB/T...
        -k*x.^2/kB/T*(lambda1(i+1)-lambda1(i));
end
x=y;
```

```
for i=1:N2
    x=x-(kk*lambda2(i)*x.^3+k*(1-2*lambda2(i))*x)*dt/gamma...
        +sqrt(2*kB*T*dt/gamma)*randn(1,n);
    WB2=WB2+kk*(lambda2(i+1)-lambda2(i))*x.^4/4/kB/T...
        -k*x.^2/kB/T*(lambda2(i+1)-lambda2(i));
end
x=y;
for i=1:N3
    x=x-(kk*lambda3(i)*x.^3+k*(1-2*lambda3(i))*x)*dt/gamma...
        +sqrt(2*kB*T*dt/gamma)*randn(1,n);
    WB3=WB3+kk*(lambda3(i+1)-lambda3(i))*x.^4/4/kB/T...
        -k*x.^2/kB/T*(lambda3(i+1)-lambda3(i));
end
```

B.5 Example 3.2 - Jarzynski relation and free energy reconstruction

```
clear all; close all; clc;
% Simulation parameters
T=300;                                  % Temperature
kB=1.38e-23;                            % Boltzmann constant
nu=0.001;                               % Viscosity of water
R=1e-6;                                 % Radius of the particle
gamma=6*pi*nu*R;                        % Friction coefficient
l=(-550:550)*1e-9;                      % Spacing
k=2e-7;
t=100e-3;
tR=.4;
dt=.1e-3;
N=round(t/dt);
lambda=sin(2*pi*(0:N)/N);
n=100000;
```

```
x=zeros(1,n);
W=zeros(1,n);




for  i=1:round(tR/dt)
     x=x-3*k*x*dt/gamma+sqrt(2*kB*T*dt/gamma)*randn(1,n);
    disp(i);
end



for  i=1:N-1
     x=x-k*(3+2*lambda(i))*x*dt/gamma...
          +sqrt(2*kB*T*dt/gamma)*randn(1,n);
     mW(i)=mean(W);
     JW(i)=mean(exp(-W));
     W=W+k*x.^2*(lambda(i+1)-lambda(i))/kB/T;
end
```